NTNU

Norwegian University of
Science and Technology

Configuration of large offshore wind farms

Randi Aardal Flo

Master of Science in Energy and Environment
Submission date: June 2009
Supervisor: Terje Gjengedal, ELKRAFT

Norwegian University of Science and Technology
Department of Electrical Power Engineering

Problem Description

The European Commission proposal for 20% renewable energy by 2020 paves the way for a massive expansion of wind energy and a new energy future for Europe. To reach the goal wind energy is a key technology and large scale integration is required both onshore and offshore. This represents heavy challenges to the power system requiring new ways of designing and operating the system. Especially large scale offshore wind power will require attention to new focus areas. The wind may be more stable offshore, but there will be less geographical smoothing effect, so wind variations will still be a key issue. Power transmission and grid connection represent other main challenges for realization of large scale wind power, and especially for offshore wind farms.

The scope of the project is defined as how to find an efficient and secure design and operation of the overall system.

The main tasks in this thesis is to study different possible configurations of a 1000 MW offshore wind farm, located 75 km from shore, and select two configurations for further study. PSS/E will be used to establish a load flow and a dynamical model of each system.

Assignment given: 02. February 2009
Supervisor: Terje Gjengedal, ELKRAFT

Preface

This master thesis is written at the Department of Electric Power Engineering at the Norwegian University of Science and Technology in cooperation with Statkraft. The work is a continuation of a project written during the autumn 2008, which dealt with transmission systems for offshore wind power.

In this thesis I have used PSS/E to make two network models of two offshore wind farm configurations with different transmission system. It took me long time to make the models, and I did not receive the HVDC Light model from ABB before May. ABB has developed a model specific DLL, so the need to compile the user models is eliminated. This new concept requires PSS/E version 31. Though, working with this thesis has been a very valuable experience.

I would like to thank Knut Magnus Sommerfelt for getting started with PSS/E, Kjetil Uhlen, professor at NTNU, for help with the modeling in PSS/E, Albert Leirbukt from ABB for help with the HVDC Light model and Kristian Stray for the good cooperation we have had. I would also like to thank my supervisor Terje Gjengedal.

Randi Aardal Flo
Trondheim, 21. June 2009

Summary

This master thesis is written at the Department of Electric Power Engineering at the Norwegian University of Science and Technology. The work has been carried out at NTNU in Trondheim. The thesis deals with configuration of large offshore wind farms and transmission systems, and is a continuation of the project written during the autumn 2008.

Today several plans on 1000 MW offshore wind farms exists. The size of the wind farms has led to a challenge of how to find an efficient and secure design of the overall system. The system has to be cost-effective in order to compete with other forms of power generation. In this study, costs is not considered.

The purpose of this thesis was to study different transmission systems and configuration of an 1000 MW wind farm located 75 km from shore. The optimal distance between the turbines is a compromise between wake effect, wind farm are and cable lengths. To perform a detailed study of wake effects and optimal spacing, computer programs like WindSim would be necessary. Three common wind farm configurations is radial, star and ring layout. The selection of layout depends on costs, wind data and the wind farm area.

Various wind turbine systems have been developed and different wind generators have been built. According to the survey of different wind generator system and considering the grid connection requirements on wind turbines, the developing trends of wind turbine generator systems shows that variable speed is very attractive and concepts with full-scale power converters will become more attractive.

In this thesis two wind farm configurations with different transmission system were further studied. AC/AC, AC/DC and DC/DC are possible transmission systems. In this thesis AC/AC and AC/DC were compared. The selected layout of the wind farm was the radial layout. Number of strings was 35, with eight turbines in each string. Each wind turbine could produce 3.6 MW, which gives a total generation of 1008 MW.

The two configurations were modeled in PSS/E. Siemens has made a model called WT3 that was developed to simulate performance of a wind turbine employing a doubly fed induction generator (DFIG). The model was developed in close cooperation with the GE Energy modeling team. This model was used in this thesis. For the dc transmission the HVDC Light from ABB was used.

Two different disturbances were applied. One at the connection point at shore, and one at the connection point for all the radials. The load flow results shows that the losses are 5.8% higher in the AC/DC system. The dynamical result shows that both of the systems were stable, and fulfill the grid code requirements. The results indicates that the short-circuit MVA is higher in the ac system than in the dc system. After a fault the voltage recovery was more smoother in the dc system, and the voltage recovery time were shorter.

Contents

List of Tables

List of Figures

1 Introduction

Wind energy is the world's fastest growing renewable energy source. The average annual growth rate of wind turbine installation is around 30% during the last 10 yeares. One of the most important economic benefits of wind power is that it reduces the exposure of our economies to fuel price volatility. The challange is that other forms of power generation is cheaper.

Offshore wind currently accounts for a small amount of the total installed wind power capacity in the world. The development of offshore wind has mainly been in northern European countries. Offshore wind capacity is still around 50% expencive than onshore wind. Although the investment cost are higher for offshore than for onshore wind farms, the total power production are higher due to higher offshore wind speeds.

Today several plans on 1000 MW offshore wind farms exists. The size of the wind farms has led to a challenge of how to find an efficient and secure design of the overall system. The development of modern wind power conversion technology has been going on since 1970s, and the rapid development has been seen from 1990s. The wind energy conversion system is demanded to be more cost-competitive in order to compete with other forms of power generation. Choice of design of the overall system is not only a question of cost, but also system stability.

This thesis is a continuation of a project written during the autumn 2008, which was an introduction to different transmission technologies for offshore wind power. The purpose of this thesis is to study different transmission systems and configuration of an 1000 MW wind farm located 75 km from shore. Two configurations with different transmission system are further studied. One with AC/AC transmission and the other with AC/DC transmission based on VSC HVDC.

PSS/E will be used for power system simulation. ABB has developed a HVDC Light model in PSS/E that will be used in this study. Load flow and transient stability will be investigated for the two different transmission technologies.

2 Wind Turbine Technology

A wind turbine is a rotating machine, which converts the kinetic energy in wind into mechanical energy. This chapter explains the main components in a wind turbine, and is mainly based on [14].

2.1 Technical overview

Figure 1 shows an overview of technical components in a wind turbine. The coming chapters explains the application of the different components.

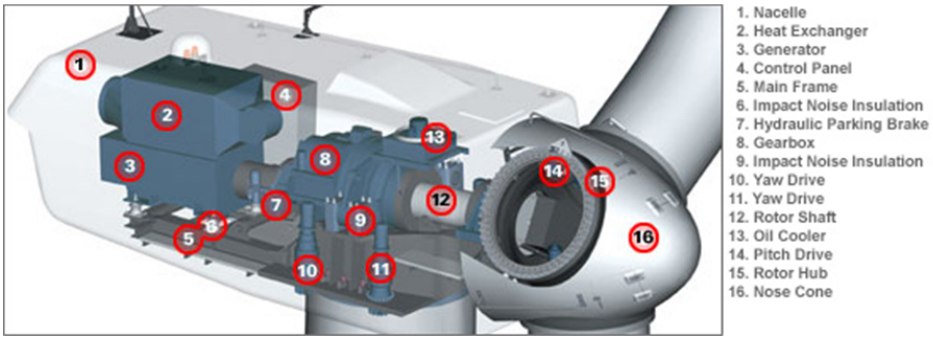

Figure 1: Technical drawing of a 3.6 GE wind turbin[4]

2.2 Rotor

The rotor consists of the hub and blades of the wind turbine. Most turbines today have upwind rotors with three blades, which means that the rotor is directed towards the wind direction. Rotors that are being developed today, seems to be built with pitch control.

2.3 Drive train

The drive train consists of the rotating parts of the wind turbine. This usually includes a gearbox, low-speed shaft, high-speed shaft, brake and the rotating parts of the generator.

2.4 Generator

All wind turbines use either induction or synchronous generator. Different wind generator systems are explained in chapter 4. The generator that has been the most commonly used so far, is induction generators. This is because induction generators are rugged, inexpensive and easy to connect to an electrical network. Without using power converters, a induction generator absorbs reactive effect.

The wind turbines can operate at fixed speed or variable speed.

2.5 Nacelle and yaw system

Nacelle and yaw system includes the wind turbine housing, the machine bed plate or main frame and the yaw orientation system. The main frame provides for the mounting and proper alignment of the drive train components. The nacelle covers the system from the surroundings. The yaw orientation system can turn the nacelle towards the most optimal wind direction. Wind direction sensor mounted at the nacelle gives signals to the yaw control system.

2.6 Pitch controlled wind turbines

Pitch-regulated wind turbines are designed for optimum power production. With pitch control the blades can be rotated about its long axis. On a pitch controlled wind turbine the turbine's electronic controller checks the power output of the turbine several times per second. When the wind power output becomes to high, it sends an order to the blade pitch mechanism which pitches the rotor blades out of the wind. Conversely, the blades are turned back into the wind when the wind drops again.

2.7 Stall controlled wind turbines

Stall-regulated wind turbines are used to regulate the aerodynamic torque at high wind speeds. The geometry of the rotor blade profile, are aerodynamically designed to ensure that the moment the wind speed becomes too high, it creates turbulence on the side of the rotor blade which is not facing the wind. The stall prevents the lifting force of the rotor blade from acting on the rotor.

3 Induction Generator

This chapter explains some basic principles with an induction generator.

3.1 Synchronous speed

The speed of the rotating flux in the stator, called synchronous speed, is directly proportional to the frequency of the supply voltage and inversely proportional to the number of pairs of poles.

$$n_s = \frac{f_s}{P/2}\, r/s \tag{1}$$

$$n_s = \frac{120 \times f_s}{P}\, r/min \tag{2}$$

where f_s is the frequency of the three-phase supply, n_s is the synchronous speed, and P is the number of poles formed by the stator windings.

3.2 Slip

The difference between the speed of the rotating stator flux and the speed of the rotor is called slip speed, and the ratio of slip speed to synchronous speed is called slip.

$$n = n_s - n_r \tag{3}$$

$$s = \frac{n_s - n_r}{n_s} \tag{4}$$

where n is the slip speed, n_s is the synchronous speed, n_r, ans s is the slip.

3.3 Power

Figure 2 shows the steady-state equivalent circuit of an induction generator. The per unit power transferred from the stator to the rotor through the air gap, called the air-gap power, is calculated from the equivalent circuit.

$$P_g = I_r^2 \frac{R_r}{s} \tag{5}$$

Subtracting the rotor losses $I_r^2 R_r$ from the air gap power, one gets the power delivered to the stator.

$$P_e = I_r^2 \frac{R_r}{s}(1 - s) \tag{6}$$

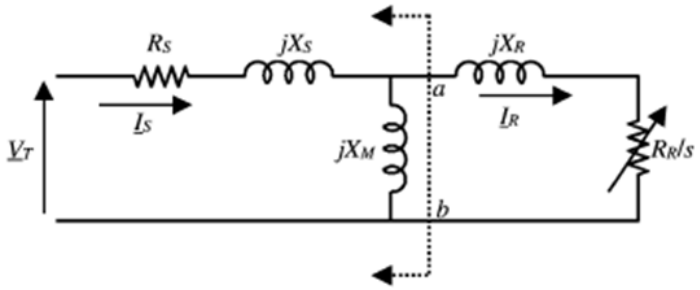

Figure 2: Steady-state equivalent circuit of an induction generator [3]

4 Wind generator systems

A significant growth of wind power capacity installed world wide has lead to a rapid development of various wind turbine concepts. The wind energy conversion system is demanded to be more cost-competitive, so that comparison of different wind generator systems are necessary. This chapter gives an overview of different wind generator systems. This chapter is mainly based on [12].

4.1 Classification of wind turbine concepts and generator types

In proportion to rotation speed, wind turbine concepts can be classified into fixed speed, limited variable speed and variable speed. Variable speed wind turbines is classified into wind generator systems with partial-scale and full-scale power converters, based on the rating of the power converter related to the generator capacity.

4.2 Fixed speed concept

Fixed-speed wind generator systems are with a multi-stage gearbox and a standard squirrel cage induction generator (SCIG), which is directly connected to the grid trough a transformer. A scheme of a fixed speed concept with SCIG system is shown in figure 3. SCIG operates in a range around the synchronous speed. The advantages of SCIG are that it is robust, easy and relatively cheap for mass production. The disadvantage is that the speed is not controllable and only variable over a very narrow range. A three-stage gearbox is necessary for the drive train for this wind turbine concept, which requires regular maintenance. And the generator always absorbs reactive effect from the grid.

Since the generator is directly connected to the grid, wind speed fluctuations are directly translated into electromechanical torque variations and periodical torque dips result in higher flicker effect. The excitation current is obtained from the stator terminal which makes it impossible to support grid voltage control.

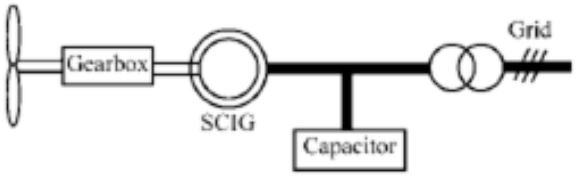

Figure 3: Scheme of a fixed speed concept with SCIG system [12]

4.3 Limited variable speed concept

The limited variable speed concept is with a multi-stage gearbox and a wound rotor induction generator (WRIG). The WRIG is with a variable rotor resistance, by means of a power electronic converter and the pitch control method. A scheme of a limited variable speed concept is shown in figure 4.

Like the fixed speed generator system, the stator is directly connected to the grid. The rotor winding is connected in series with a controlled resistor. To achieve variable-speed operation the energy extracted from the WRIG rotor is controlled, but this power must be dissipated in the external resistor. The variable speed range depends on the size of the variable rotor resistance, and is typically less than 10% above the synchronous speed.

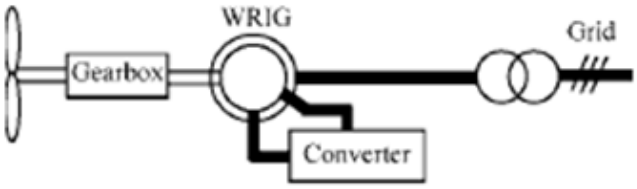

Figure 4: Scheme of a limited variable speed concept with WRIG system [12]

4.4 Variable speed direct-drive concept with a full-scale power converter

In this concept the direct-drive generator is connected to the grid through a full-scale power converter. Direct-drive means that the generator rotor is directly connected to the hub of the turbine rotor, which cause a low generator rotor speed. To be able to deliver a certain power, the lower speed makes it necessary to produce a higher torque, which requires a larger size of the generator. This is obtained by using multi-poles. Larger number of poles requires a larger diameter for implementation with a reasonable pitch. The advantages of direct-drive wind turbines is high overall efficiency, and high reliability and availability by omitting the gearbox.

Direct-drive generators used in the market can be classified into electrically excited synchronous generator (EESG) and the permanent magnet synchronous generator (PMGS).

4.4.1 Electrically excited synchronous generator

Electrically excited synchronous generator is usually built with a rotor carrying the field system provided with a DC excitation, and the stator carries a three-phase winding. Figure 5 shows a grid connection scheme of EESG for direct-drive wind turbines.

The converter at the generator side can control the amplitude and frequency of the voltage, so that the generator speed is fully controllable over a very wide range. The converters at the rotor side can control the excitation current, which controls the flux. Though, this solution is heavy weighted and expensive. Another disadvantage is that it is necessary to excite the rotor winding with dc, using slip rings and brushes, or brushless exciter, employing a rotating rectifier, and the field losses are inevitable.

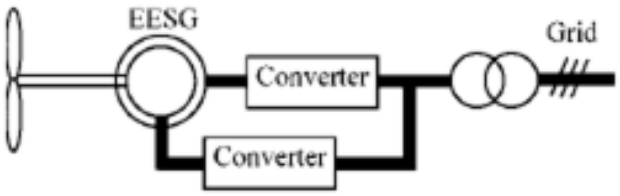

Figure 5: Scheme of a direct-drive EESG system [12]

4.4.2 Permanent magnet synchronous generator

Figure 6 shows a grid connection scheme of PMGS for direct-drive wind turbines. Permanent magnet synchronous generators are widely used in variable-speed wind generators for their high performance. The main reason relay on their optimal characteristic, which are higher efficiency and higher generated power-weight ratio than induction generators. Power losses are mainly related to the stator windings and the stator core because the rotor is loss-free.

One of the disadvantages is that the cost of permanent magnet material is very high. But in recent years, the use of PM is more attractive than before, because the performance of permanent magnets is improving and the cost is decreasing.

4.5 Variable speed single-stage geared concept with a full-scale power converter

This system is an extended concept of the variable speed direct-drive concept with a full-scale power converter. The difference is that a variable speed pitch control wind turbine is connected to a single-stage planetary gearbox, that increase the speed by a

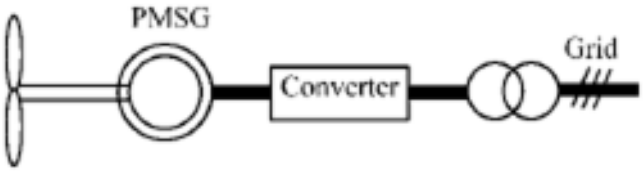

Figure 6: Scheme of a direct-drive PMSG system [12]

factor of roughly 10. The generator and a low-speed permanent-magnet generator. This concept has the advantages of a higher speed than the direct-drive concept, and a lower mechanical component than the multiple-stage gearbox concept. Figure 7 shows a grid connection scheme of PMGS for single-stage geared wind turbines.

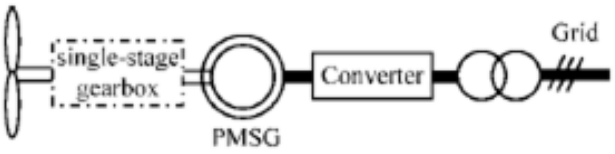

Figure 7: Scheme of a single-stage drive PMSG system with a full-scale converter [12]

4.6 Variable speed multiple-stage geared concept with a full-scale power converter

In proportion to the concept explained in chapter 4.5, this concept is with a multiple-stage geared concept instead of single-stage geared concept. Variable speed multiple-stage geared concept is developed with PMSG and SCIG system.

4.6.1 PMSG system

A PMSG system is used in order to reduce the generator's volume and improve the generator efficiency in variable speed wind turbine concepts with a full-scale power converter. Compared with the DFIG system, that will be explained in chapter 4.7, the generator in this system has a higher efficiency and it is not necessary with brushes. The grid-fault ride-through capability is less complex. But the disadvantages is that the converter is larger, more expensive and the losses are higher because all the power are processed by electronic converter. Figure 8 shows a grid connection scheme of PMSG for multiple-stage geard wind turbines.

Figure 8: Scheme of a single-stage drive PMSG system with a full-scale converter [12]

4.6.2 SCIG system

Variable speed multiple-stage geared SCIG with full scale converter is shown in figure 9. Compared with the fixed speed concept, the difference is the full-scale power converter. The converter gives the possibility to variable speed operation, reactive power compensation and better smooth grid connection. However, the system is more expensive and high losses in the converter leads to a lower efficiency of the total system.

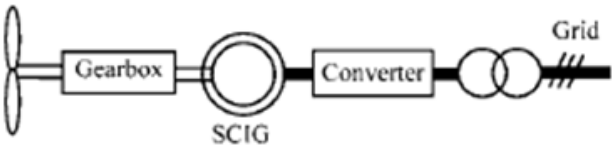

Figure 9: Scheme of a direct-drive EESG system [12]

4.7 Variable speed concept with partial-scale power converter

This configuration is known as the doubly fed induction generator system (DFIG). Figure 10 and figure 11 shows a grid connection scheme of a variable speed concept with DFIG system. The generator is a WRIG with the stator connected directly to the grid, and the rotor is connected trough a power electronic converter. The converter is typically rated at around 25-30% of the generator rating for a given rotor speed range of about 30% of synchronous speed. While the rotor speed varies the DFIG can supply power at constant voltage and constant frequency [19]. The converter is a partial-scale back-to-back converter, which is a four-qadrant converter. Therefore the DFIG can produce or absorb an amount of reactive power.

If the stator and the rotor losses are neglected, the power through the converters, slip power, can be expressed as slip, s, multiplied by the stator power, P_{stator} [19].

$$P_{rotor} = sP_{stator} \tag{7}$$

$$P_{stator} = \frac{1}{(1-s)P_{gr}} = \frac{\eta_g P_m}{1-s} \tag{8}$$

where η_g is the generator efficiency and P_m is the mechanical power.

Compared with fixed speed generators, DFIG offers more advantages such as speed control, reduced flicker, and four-quadrant active and reactive power capabilities. However, this concept also use gearbox and slip rings as well, which requires regular maintenance. Other disadvantages are large rotor currents resulted by large stator currents under grid fault conditions, and complicated control strategies because of grid connection requirements that requires a ride-through capability. Compared with a full-scale converter, the full scale power converter can perform smooth grid connection over the entire range. Since the total amount of generated power has to pass the through the power converter, it has higher losses. A full-scale converter is also more expensive.

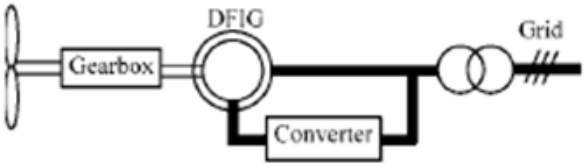

Figure 10: Scheme of a direct-drive EESG system [12]

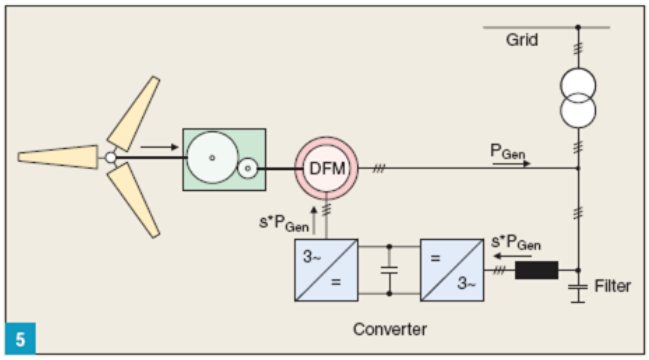

Figure 11: Scheme of a direct-drive EESG system [23]

4.8 Market trends

Different companies produces various types of wind turbines with different power rating and concept. Most manufactures are using geared-drive wind turbine concepts, and the the market is still dominated by DFIG with multiple-stage gearbox. But PM machines becomes more and more attractive because of the higher efficiency and energy yield, higher reliability and the cost has decreased in recent years.

5 Wind farm grid interface

Power system stability is defined as that property of a power system that enables it to remain a state of operating equilibrium under normal operating conditions and to regain an acceptable state of equilibrium after being subjected to a disturbance [15]. Norwegian Water Resources and Energy Directorate (NVE) have given Statnett the responsibility to protect satisfactory delivery quality, operation, and efficient utilization of the power system. Statnett have published a rapport that describes the system requirements to all network owners and power producers [6]. The first part of this chapter describes the requirements that are important to producers of wind power. The rest of this chapter explains some power system stability phenomenas, which is mainly based on [15].

5.1 System requirements

Below is a list of the most important requirements in proportion to wind farms.

- wind farms have to operate continuously within the voltage of 0,90-1,05 pu at 49,0-52,0 Hz, and at the frequency of 47,5-49,0 Hz within less than 30 min
- wind farms must have a mutual regulator to control the active power production from shore
- the active power production in normal operation should not be limited to regulate the frequency in case of low frequency
- the adjustment of the regulator speed must be able to operate within 10-100 % of rated power/min
- the reactive power capacity must be $\cos(\varphi) = \pm 0,95$ at the point of grid connection at rated production

Also during faults there are some requirements. The power plants shall contribute to short-circuit power during faults, and maintain connected during faults. This requirement is referred to as the *fault ride trough* (FTR). Power plants that are connected to a directly grounded grid with nominal voltage greater than 200 kV should operate and deliver power when the voltage at the connection point has the following voltage profile:

- Voltage reduction to 0% voltage up to 150 ms
- Followed by voltage increase to 25%
- Followed by a linear voltage increase from 25% to 90% within 750 ms
- Followed by constant voltage 90%

The voltage profile is shown in figure 12.

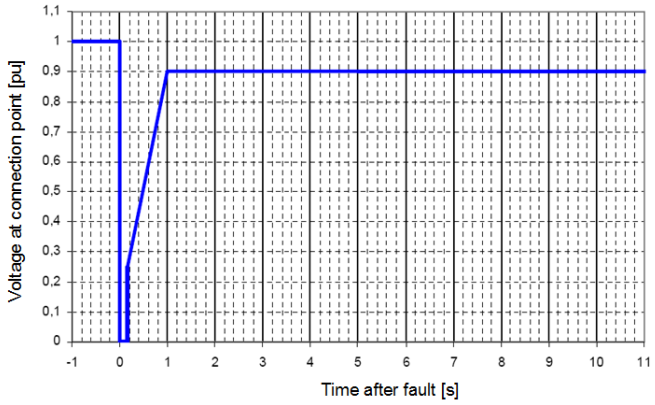

Figure 12: Fault ride trough requirement for power plants with voltage greater than 200 kV [6]

5.2 Transient Stability

Transient stability is the ability of the power system to maintain synchronism when subjected to a severe transient disturbance. Such disturbances are short-circuits of different types like phase-to-ground, phase-to-phase-to-ground, or three-phase. The resulting system response involves large excursion of generator rotor angles and is influenced by the nonlinear power-angle relationship.

5.3 Voltage Stability

Voltage stability is the ability of a power system to maintain steady acceptable voltages at all buses in the system under normal operating conditions. Voltage instability occurs if a disturbance, increase in load demand or change in system condition causes a drop in voltage.

If the one of the bus voltage magnitude decreases when the reactive power injection at the same bus is increased, the system is voltage unstable. This is the same if the V-Q sensitivity is negative for at least on bus, the system is unstable. The main reason for instability is the high demand of reactive power and if the system is not able to meet this demand. Voltage instability may lead to voltage collapse, which is a result of a sequence events of voltage instability leading to a low-voltage profile in a major part of the power system. Figure 13 shows the relationship between P and V. The active power corresponding to the critical voltage is the maximum power before voltage instability.

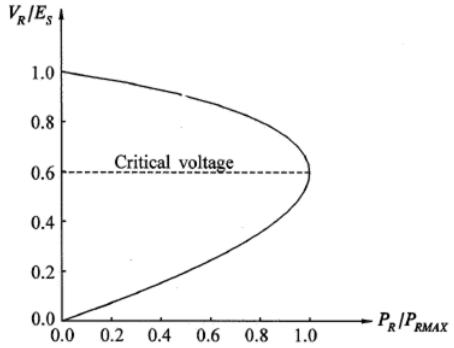

Figure 13: Power-voltage characteristics of a system, cos(ϕ)=0.95 lag [15]

6 AC transmission

This chapter gives an overview of characteristics of AC transmission that effect the system stability and voltage control. The last part of this chapter explains AC system strength, which is relevant regarding connection of offshore wind power. This chapter is mainly based on [15].

6.1 Overhead lines

A transmission line is characterized by four parameters: series resistance R due to the conductor resistivity, shunt conductance G due to leakage currents between the phases and ground, series inductance L due to magnetic field surrounding the conductors, and shunt capacitance C due to the electric field between conductors. The shunt conductance represents losses due to leakage currents along insulator strings and corona. Usually it is neglected because its effect is small.

6.2 Power transmission

A underground cable have the same parameters as overhead lines. Because of the difference in design and distance between the conductors, the values of the parameters and so the characteristic of cables differs from overhead lines.

6.3 Surge impedance load

A transmission line and a cable can be described by their *characteristic impedance* Z_C, which is given by

$$Z_C = \sqrt{\frac{R + j\omega L}{j\omega C}} \approx \sqrt{\frac{L}{C}}(1 - j\frac{R}{2\omega L}) \tag{9}$$

The shunt conductance is neglected. Since the resistance is usually small, high-voltage lines are assumed to be lossless when dealing with lightning and switching surges. If the

losses are neglected the characteristic impedance Z_C is referred to as the *surge impedance*. The power delivered by a transmission line when it is terminated by its surge impedance is known as *natural load or surge impedance load* (SIL), which is given by

$$SIL = \frac{V_0^2}{Z_C} \quad W \tag{10}$$

where V_o is the rated voltage of the line. At natural load, the reactive power generated by the shunt capacitance is equal to the reactive power absorbed by the series inductance, for each incremental length of the line. If the line is loaded below SIL, the line will produce reactive effect. Hence, the shunt capacitance is larger than the series inductance. Opposite, if the line is loaded above SIL, the line will absorb reactive effect. The series inductance is then larger than the shunt capacitance. For a transmission cable, the shunt capacitance is usually larger than the series inductance, and will therefore produce reactive power.

6.4 Short-Circuit Ratio

The ac system can be considered as "weak" from two aspects: ac system impedance may be high and ac system mechanical inertia may be low. Strength of the ac system has a very significant impact in the ac/dc system interactions. The relative strengths of ac systems is given by *short-circuit ratio* (SCR).

$$SCR = \frac{short - circuit\ MVA\ of\ ac\ system}{dc\ converter\ MW\ rating} \tag{11}$$

The short-circuit MVA is given by

$$SC\ MVA = \frac{E_{ac}^2}{Z_{th}} \tag{12}$$

E_{ac} is the bus voltage at the connection point at rated dc power and Z_{th} is the Thevenin equivalent impedance of the ac system seen from the connection point. Short-circuit MVA is the short-circuit power in the connection point. SCR=4,5 is very high and SCR=1,5 is very low [8]. The problem with low short-circuit MVA, is that the current during a fault is to low, so the over-current relay will not react on the fault. In case the protection device does not react, the fault will not be removed.

Conventional HVDC requires a strong network to commutate [16]. VSC are self-commutating converters, explained in chapter 7, that control both active and reactive output power, and is therefore suitable for weak networks. Since VSC can supply reactive effect it may contribute some short-circuit current [30].

Another measure of the interaction between ac and dc systems is the effective inertia constant. To maintain the required voltage and frequency in a ac system, the system should have a minimum inertia relative to the size of the dc links. The effective inertia constant is given by

$$H_{dc} = \frac{totalrotational\ inertia\ of\ ac\ system\ [MW \bullet s]}{MW\ rating\ of\ dc\ link} \tag{13}$$

H_{dc} is recommended to be at least 2.0 to 3.0 for satisfactory operation.

7 HVDC Light

In 1997, ABB introduced a completely new converter and DC cable system called HVDC Light, based on voltage source converter (VSC) technology. The HVDC Light system provides exact control of active power transmission. The power transmission can be combined with a frequency converter that varies the power to support the network frequency. Being relatively compact and lightweight, and with its superior control properties, VSC technology is therefore suitable for supplying electrical power from shore to offshore installation.

7.1 Converter technology

HVDC Light is based on Voltage Source Converters (VSC) that include Insulated Gate Bipolar Transistors (IGBT's) and operate with high frequency Pulse Width Modulation (PWM) in order to control both active and reactive power. The HVDC Light system is shown in figure 14.

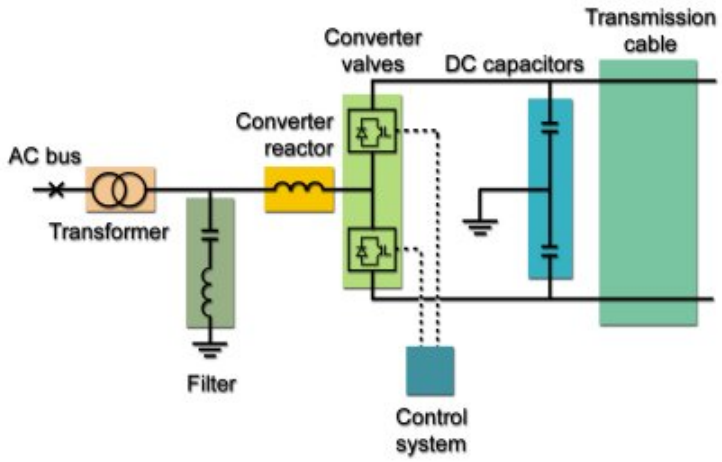

Figure 14: The HVDC Light system [9]

The converter consists of an IGBT valve bridge, the converter control, the converter reactor, DC capacitor and an AC-filter. The bridge is in its basic form a two-level, three-phase topology with six valves and series connected IGBT's in each valve. The number of devices required is determined by the rated power of the bridge and the power handling capability of the switching devices [5]. VSC are self-commutated converters [20]. This means that the valves does not need any voltage on the load side of the converter to commutate. The VSC does not have to be connected to a stiff network so it is possible to supply a system without any rotating machines [25]. The VSC is shown in figure 15.

Every IGBT is provided with an anti parallel diode so the current can flow in both directions. Turn on/off of each single IGBT is ordered via an optical link from the control equipment on ground potential. The semiconductors are cooled with deionized water [9].

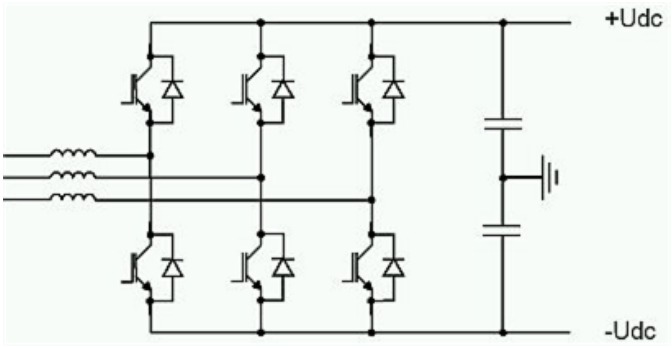

Figure 15: The main circuit of the VSC [9]

7.2 Pulse-Width-Modulation

In inverter mode PWM is used to produce a sinusoidal output voltage waveform. With PWM it is possible to create any phase angel or amplitude (up to a certain limit) by changing the PWM pattern, which can be done almost instantaneous [9]. The active and reactive power can therefore be controlled independently. The PWM pattern and the fundamental frequency voltage is shown in figure 16.

The sinusoidal output voltage consist of the fundamental frequency AC component plus higher-order harmonics. To filter the high-order harmonics a passive high-pass AC filter is used. The series converter reactor is necessary to separate the AC fundamental frequency from the raw PWM waveform [9]. The DC capacitor smooths the DC-voltage and the DC-filter eliminates harmonics on the DC side of a converter.

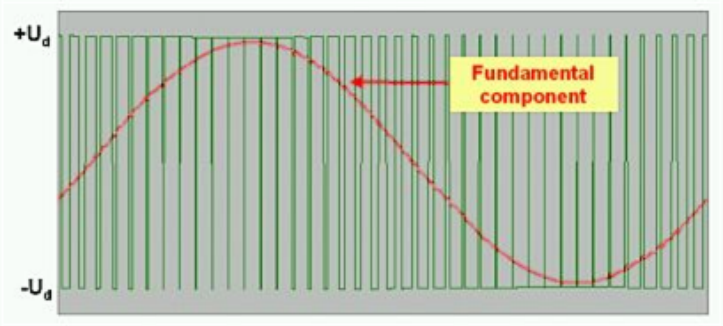

Figure 16: The PWM pattern and the fundamental frequency voltage [9]

7.3 Cables

The new HVDC Light cables have insulted extrude polymer, mostly XLPE. This makes it more strong and robust so it can be laid in deeper waters and on rough bottom. The cables are operated in bipolar mode which eliminates the magnetic fields.

7.4 Capability

The system apparatus capability is a common way to show under what conditions it can operate safely. It is mainly two factors that limit the active and reactive power output from an HVDC Light. This is the maximum current passing the IGBT-transistors and the maximum DC-voltage. Rated MVA capacity is given by voltage times current. Since HVDC Light is a voltage source converter it can not raise the AC voltage above a certain level [9]. The level i restricted by the maximum DC-voltage allowed on the DC apparatus. Figure 17 shows how the limits vary with voltage. From the figure it can be seen that the voltage defines the maximum absorbed reactive power. The maximum rated active power of a HVDC Light is 1200 MW [9].

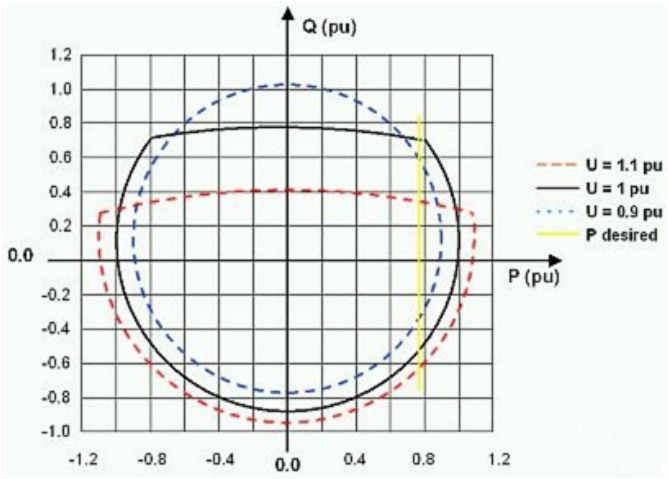

Figure 17: [9]

7.5 Stability

Voltage drops is usually caused by increase in load demand. The ability of VSC HVDC to control reactive and active power output improves the voltage stability in the network. [13],[9] shows that VSC HVDC in different network transmission systems can enhance to transient stability, to improve power oscillations damping, and to improve voltage support. This is because HVDC VSC can rapidly control the transmitted power and independently exchange reactive power with transmission systems. Next chapter explain the definitions of stability in power systems more deeply.

7.6 Multi terminal

To connect several transmission systems require the connection of more than two terminals to a common DC-bus, called multi-terminal dc (MTDC) schemes. This is relevant for clustering of wind farms or combining offshore wind farms to oil and gas platforms and wave and tidal energy. VSC HVDC is suitable for MTDC [29]. The converters regulates

the amount of power fed into or absorbed from the ac system and the power-frequency control can be maintained by the dc system.

8 Configuration of offshore wind farms

Today it exist several plans on 1000 MW wind farms. These large wind farms are mainly considered to be located out in the sea. The problem with such large wind farms is to find an optimal design of the park. In this chapter different possible configuration of wind farms are presented and evaluated.

8.1 Electrical system configuration

In this part, different electrical configurations for the wind farm are described. This part is mainly based on [17].

8.1.1 AC/AC layout

Figure 18 and 19 shows the electrical system for a small and a large AC wind farm. The small AC system is suitable for small wind farms and short transmission distances. In the large AC system the wind turbine radials are connected to a transformer and a high voltage transmission system connected to PCC (point of common coupling). Since the transmission distance is longer, this system requires an offshore platform for for the transformer and switch gear.

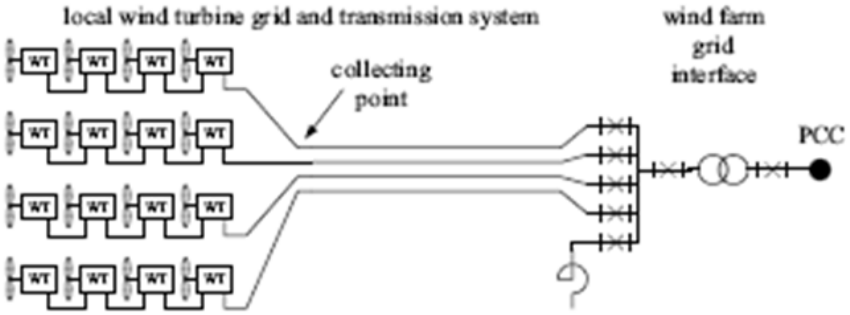

Figure 18: Electrical system for a small AC wind farm [17]

8.1.2 AC/DC layout

Figure 20 shows the electrical system for a AC/DC wind farm. Compared with the large AC/AC system, the high voltage AC transmission is replaced with high voltage DC transmission in this system. When transmission distances exceeds 100-150 km HVDC transmission may be the only feasible option for connection of wind farms [16].

As discussed in chapter 7, HVDC Light can control both the voltage and frequency which makes it more suitable to connect the wind farm to a weak network.

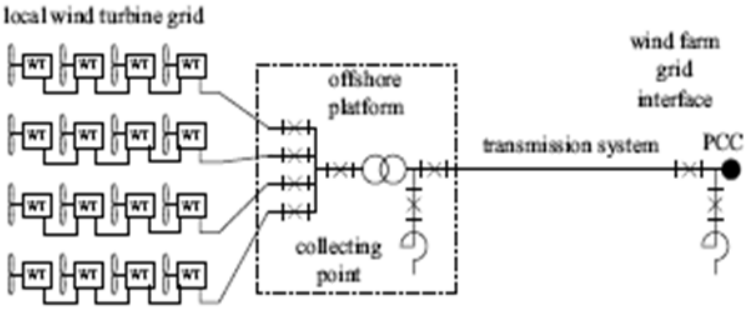

Figure 19: Electrical system for a large AC wind farm [17]

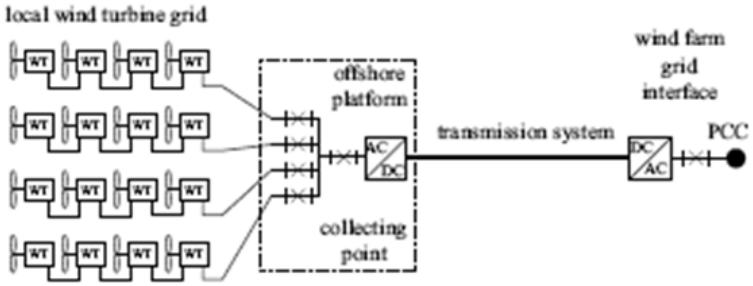

Figure 20: Electrical system for a AC/DC wind farm [17]

8.1.3 DC/DC layout

Figure 21 and 22 shows the electrical system for a small and a large DC/DC wind farm. The electrical configuration for the small DC system is identical to the small AC wind farm. But instead of the transformer in the wind farm grid interface it is replaced with a DC transformer and inverter. A rectifier is of course needed in each wind turbine.

The difference between the large AC and the large DC configuration is if the DC configuration requires one or two transformations steps. If the DC voltage from the wind turbines is lower than 5 kV, a second transformer step is required to increase this voltage. This configuration is presented in figure 22. If only one step is used, the wind turbines are connected in radials directly to the second DC transformer step.

Another possible configuration is with the wind turbines connected in series. Figure 23 shows the electrical system for this configuration. By connecting the wind turbines in series and transform the voltage in the local DC/DC converter in each wind turbine, it is not necessary with a large DC-transformers and offshore platforms. The disadvantages with a configuration like this, is that the DC/DC converters in the wind turbines must have the capability to operate towards a very high voltage. In case on of the wind turbines are disconnected, the other turbines must compensate for this and increase their output voltage.

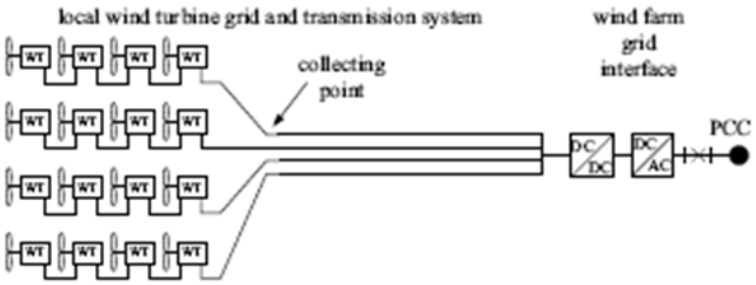

Figure 21: Electrical system for a small DC/DC wind farm [17]

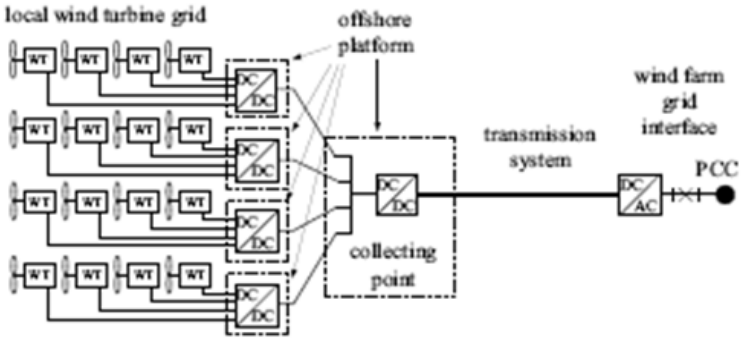

Figure 22: Electrical system for a large DC/DC wind farm [17]

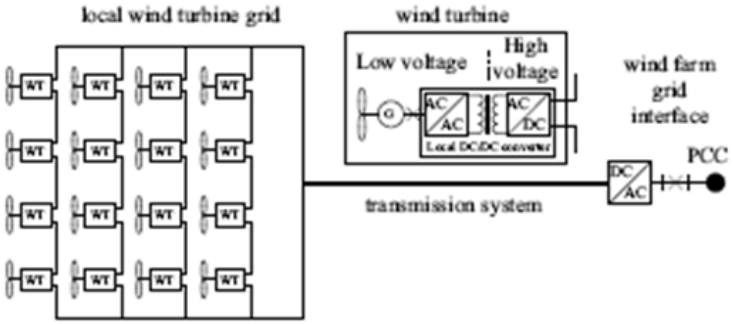

Figure 23: Electrical system for a DC/DC wind farm with series connected wind turbines [17]

8.2 Wake effects

Electric power produced by wind turbines is generated by extract the energy in the wind. Accordingly, the wind speed must be lower behind the wind turbines which is so-called wake effect. Blade geometry, pitch angle, rotor speed and so on will affect the wake effect. This makes it difficult to foresee the exact output performance of the wind before it is actually in operation. Studies shows that the general pattern is that the power output decreases significantly from the first to the second turbine, and then decreases steadily, but in smaller steps, towards the last wind turbine. To avoid this, the wind farm can be made longer and more stretched out instead of quadratic, so more of the wind turbine placed in the back rows will be moved to the front area.

8.3 Distance between the wind turbines

It is common for offshore wind turbines to be spaced between five and nine rotor diameters [27]. If the wind turbines are located to close to each other, the wind will be more and more turbulent after it passes each turbine. This leads to higher aerodynamical stresses subjected to the turbines [17]. Higher distance between the wind turbines increases the total area that the wind farm occupies and also the cable distances. The optimal distance between the turbines is a compromise between wake effect, wind farm area and cable lengths. To perform a detailed study of wake effects and optimal turbine spacing, computer programs like WindSim would be necessary.

8.4 Wind farm configuration

In this section three common wind farm configurations will be presented. These three are the radial, ring and star solution.

8.4.1 Radial configuration

Figure 24 and 25 shows two possible configurations of the radial solution. The average wind direction and velocity is supposed to be directed towards the long side on the opposite side of the offshore transformer platform. This will minimize the wake losses and

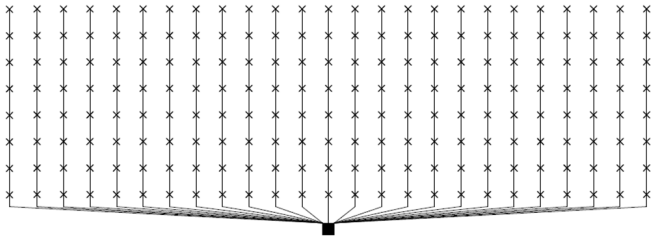

Figure 24: Example 1 of wind farm configuration with radial structure [27]

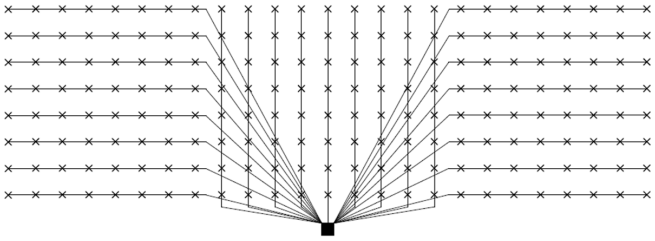

Figure 25: Example 2 of wind farm configuration with radial structure [27]

Both of these configurations are suitable if the wind direction and velocity is directed towards the long side on the opposite side of the offshore transformer platform. This will minimize the wake losses. Example 1 has a very symmetric form, so the wake effect becomes less along the rows, and power will be almost equally distributed in each string. Example 2 has shorter cable lengths that will reduce cable costs and power losses. This configuration will not have equally distributed power in each string. Because of wake effects, strings that connect the foremost wind turbines will have almost constantly high power output. Another difference is that the cables laid inside the wind farm in example 2 are crossing each other, which might complicate reparations and so on.

8.4.2 Ring layout

Ring or closed loop arrangement is an extended configuration of the radial system. Two strings are connected in a a ring arrangement. Figure 26 shows the ring arrangement. A cable connecting each string at the end would provide redundancy in the event of failure at some point in the string. Then a faulty cable segment could be isolated and operation could continue without any loss of generation. Compared to the radial configurations, ring arrangement requires greater conductor cross-section. The probability of a fault in

a buried submarine cable is low, 0.1 faults per year per 100 km [22]. Therefore the slight of improvement in reliability will probably not even out the added cable costs [18].

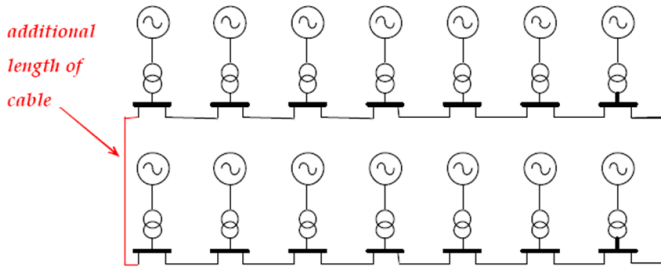

Figure 26: Two strings connected in a ring arrangement [18]

8.4.3 Star configuration

In star configuration 9 wind turbines can be placed in a 3x3 formation, and each wind turbine is connected to a cable that transfers the power to the windmill in the center of the star where the transformer is placed. Compared with the radial configuration, the voltage is not transformed in each wind turbine but in the center of the star. This will probably increase the power losses. However, there is no need for a separate transformer connected to each windmill. Figure 27 and 28 shows two possible configurations of the star solution.

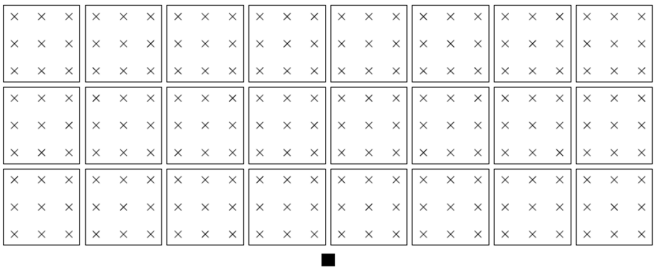

Figure 27: Example 1 of wind farm configuration with star structure [27]

In example 2, two of the stars are removed and the offshore platform is moved into this area. This reduces the cable lengths. But on the other hand, the risk of ships collide with the wind turbines during repair of the platform is higher in this configuration.

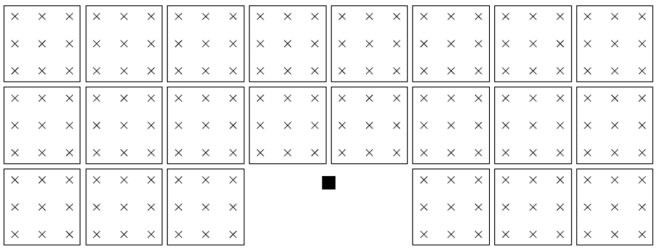

Figure 28: Example 2 of wind farm configuration with star structure [27]

9 Selection of system configuration

It is very difficult to find an optimal configuration of the overall system i an large offshore wind farm. Because this depends on many factors that can be optimized for separately, but an total evaluation is more complicated. This chapter presents the selected configurations.

9.1 Wind generator system

Chapter 4 describes different wind generator systems. For offshore wind turbines it is much more important to be robust and maintenance free, because the it is extremely expensive and difficult and even impossible to do offshore maintenance and reparations under some weather conditions.

Fault ride-trough capability is required to avoid losses of wind power production during a grid fault, and should also be taken into consideration. Higher efficiency will give an higher energy output. Cut-in and cut-off speed will also influence the annual energy output because it effect the available operational time of wind turbines. [12]

In this study, the DFIG concept was selected. According to [12] is the multiple-stage geared-drive DFIG concept still the dominant in the current market. [12] also refers to [7] which concludes that the direct-drive system would be more expensive and heavier than the DFIG wind turbines. Although systems with full-scale power converters are not directly connected to the network and may be less complicated to deal with grid-related problems, and these may be more effective. Systems without a gear needs also less maintenance.

A GE 3.6 MW doubly-fed induction generator is used in this study, because the PSS/E wind turbine model is based on wind turbines delivered by GE Energy. This model is described in chapter 10.1. For GE 3.6 applications, the transformer will typically be 34.5kV/4160V. Based on Norwegian voltage levels 34.5kV is set to 33kV.

9.2 Wind farm configuration

Chapter 8 describes different wind farm layouts. To avoid wake effects, the wind farm can be made longer and more stretched out instead of quadratic, so more of the wind turbine placed in the back rows will be moved to the front area. Choice of wind configuration

depends on wind data and different area has different wind data. In this study this is not taken into concern. Therefore the selected configuration is based on the radial layout in figure 24.

It is common for offshore wind turbines to be spaced between five and nine rotor diameters citekonf. In this study six rotor diameters are used. Rotor diameter of the GE 3.6 WTG is 104 m [4].

Each radial connects eight wind turbines. A higher number of turbines means longer cables and higher losses. A larger conductor cross-section is also required because a higher amount of power is transferred. Fewer turbines gives several radials and longer distance to the offshore platform. However, in case of a fault in one of the radials, the loss of power production would be less if a lower number of turbines in each string. A lower number of wind turbines in each string also avoid wake effect. Number of turbines in each string is also a question of economy, wake effect and also the probability of grid faults.

Since the selected wind turbine has a rated prower of 3.6 MW, the number of radials is 35 which gives a total power generation of 1008 MW.

9.3 Transmission system

Chapter 8.1 describes different electrical configurations of a wind farm. The size of the wind farm is 1008 MW and the transmission distance to shore is 75 km. It is therefore necessary with an offshore transformer platform. In this thesis AC/AC and AC/DC transmission is selected and compared. Because the development of this technology has been going on for a long time.

ABB has developed an AC/DC converter, HVDC Light, which is explained in chapter 7. ABB has also made a PSS/E model of HVDC Light. This model is used in this thesis, and is explained in chapter 10.5.

The maximum power generated by the wind turbines is 1008 MW. In case a fault on the cable to shore, will in worst case give a loss of 1008 MW. Several cables gives higher reliability. In this thesis the number of AC transmission cables is two and the HVDC Light system is a bipolar system.

9.4 Transformer

Numbers of transformers at the offshore platform varies and depends on the generated power. Several transformers give a more reliable system. If a transformer breakdown, the repair time is long. This will result loss in generation if not the other transformers are over sized.

The transformers at the offshore platform were modeled as one large transformer with a rated power of 1200 MVA. This made the model more simple and analyzing transformer breakdown was not of interest in this thesis.

The HVDC Light system operates at 320 kV DC voltage (pole to ground), and the voltage level of the transformer is set to 400/416 kV. The voltage level of the high voltage AC transmission system was set to 420 kv because higher voltage gives less power losses.

9.5 Sizing of cables

Larger conductor cross-section gives less losses and the power rating is higher, but it is more expensive. When sizing cables it is often preferred to size the largest cable first i.e. the one carrying the most power and work "*backwards*", sizing the intermediate and small cables last [18].

The maximum generated power by each radial is 28.8 MW, and all the eight wind turbines can absorb or produce maximum 13.92 MVAr. The cables also produce some reactive power. The largest cable must at least have an power rating of 32 MVA.

Technical cable data for 33 kV XPLE submarine cables, delivered by ABB, are given in table 1. The data are found in [18] and [10]. The rated values are based on solid Cu conductor. Ratings are calculated for a 1.0 burial depth with 1.0 K· m/W and sea temperature no higher than 20^0C. Table 2 is data given for 36 kV cables, but it is assumed that the data are the same for 33 kV cables. The data are found in [11].

Table 1: 33 kV submarine cable data

Conductor CSA $[mm^2]$	Conductor resistance AC 90^0C $[ohm/km]$	Inductance $[mH/km]$	Current rating $[A]$	Power rating $[MVA]$
120	0.20	0.41	325	18.6
150	0.16	0.40	365	20.9
185	0.13	0.38	449	25.7
240	0.10	0.37	513	29.3
300	0.08	0.36	572	32.7
400	0.06	0.35	637	36.4
500	0.05	0.33	659	39.7
630	0.04	0.32	776	44.4
800	0.03	0.31	838	47.9

Table 2: Capacitance for 36 kV cables [11]

Conductor $[mm^2]$	Capacitance $[\mu F]$
120	0.18
150	0.20
185	0.21
240	0.23
300	0.25
400	0.28
500	0.31
630	0.34
800	0.38

Table 1 states that the maximum power of a cable of 400 mm^2 can support 36.4 MVA.

This cable can safely support eight wind turbines linked together. The largest cable are connected between the offshore platform, and links the first and the second wind turbine. The cables in each radial was divided in three different sizes. The following three cables, from the second wind turbine, must have a cross-section of 240 mm^2. The three last cables must support three wind turbines, which correspond to a maximum power of 12 MVA. Table 1 states that the smallest cable has a conductor cross-section of 120 mm^2 and can support 18.6 MVA. The cables are a bit over sized, but smaller cables gives also higher power losses.

Cable data for the high voltage DC transmission cables are given in chapter 10.5. The technical cable data for the HVAC transmission cable is 0,064+j0,1031 Ohm/km and shunt capacitance=0,13μF/km. This is data for a 300 kV AC cable with rated power of 550 MW. The cable data was used, even though the voltage level is 420 kV.

9.6 Single line diagram

Figure 29 and 30 shows the single line diagram of the two selected configurations. It can be seen from the figures that not all of the radials is modeled as strings with eight wind turbines. These are modeled with one wind turbine, one transformer and connected to the offshore transformer platform. This was done since all the strings are equal. How the equivalent is modeled is explained in chapter 10.3.

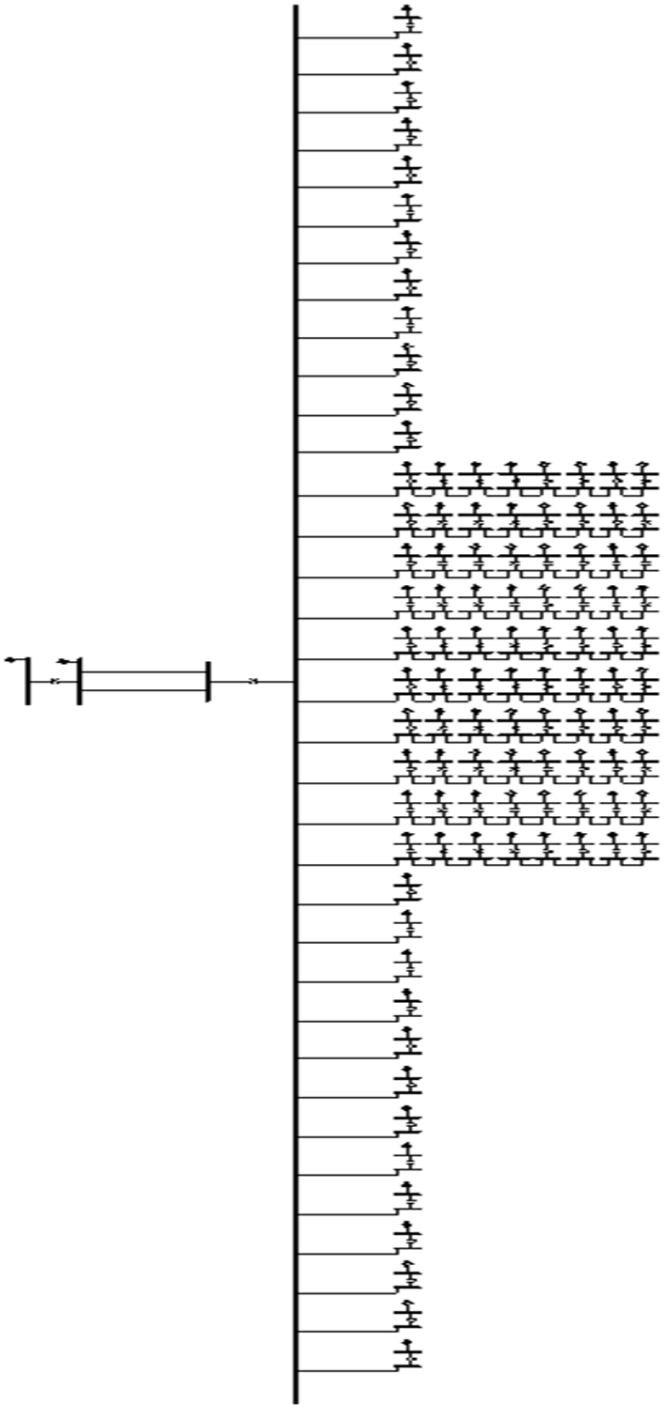

Figure 29: Single line diagram of the AC/AC system

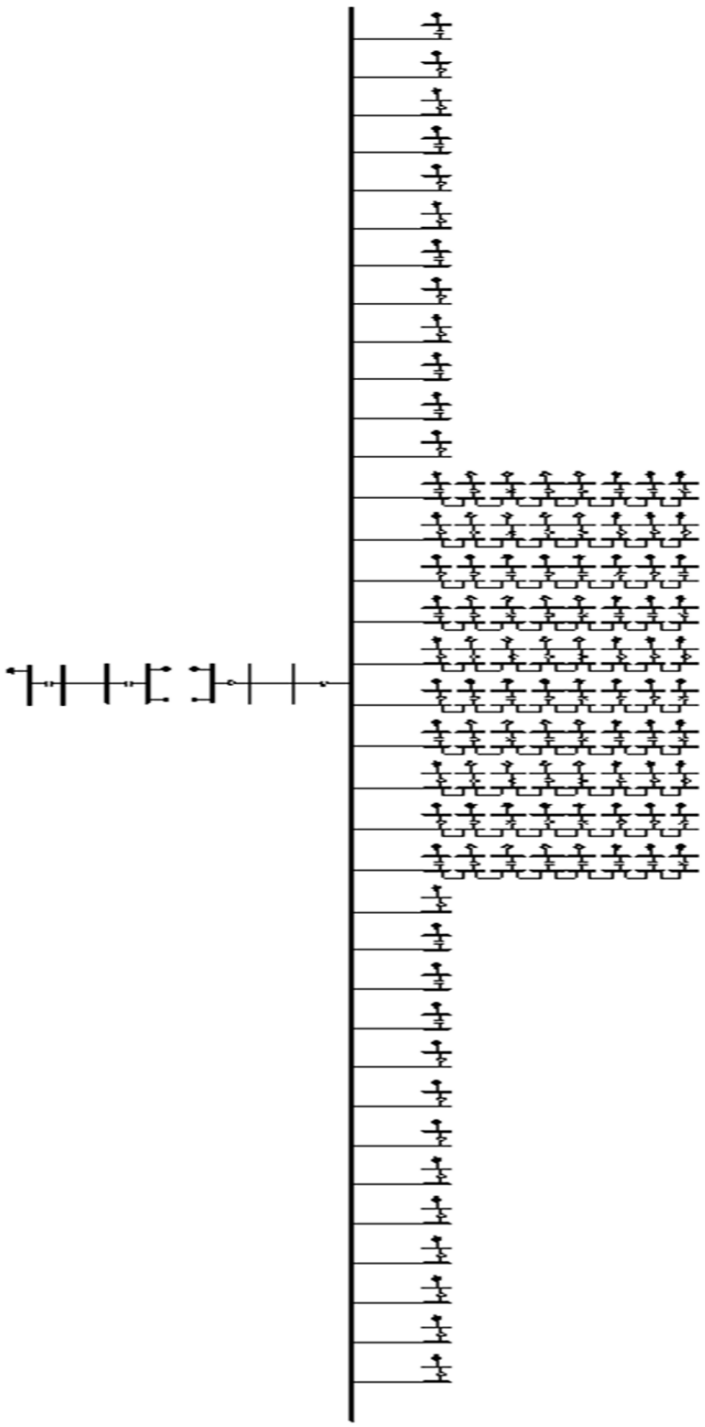

Figure 30: Single line diagram of the AC/DC system

10 Modeling

This chapter describes how the two selected configurations are modeled. There are several programs available to preform load flow and dynamical analysis of a power system. In this thesis was PSS/E used. PSS/E is owned by Siemens.

10.1 GE 3.6 Wind Turbine-Generators

Siemens has made a model called WT3 that was developed to simulate performance of a wind turbine employing a doubly fed induction generator (DFIG). The model was developed in close cooperation with the GE Energy modeling team. [21] contains most of the parameters of a GE 1.5 and 3.6 MW wind turbine-generator. The data is given for a 60Hz GE 3.6 wind turbine. The frequency in this study is 50 Hz, but the same technical data are used. At Siemens web page it is possible to download updated versions of the wind turbine models from GE. Since this became familiar relatively late during this study, most of the parameters is taken from [21]. Rest of the parameters is taken from the PSS/E manual [24] that describes the WT3 model, which contains parameters of an updated version of a GE 1.5 MW wind turbine-generator. These are parameters are assumed to be independent on rated power.

In PSS/E you have to make a load flow model and a dynamical model. The dynamical wind turbine model consists of four device modules, generator/converter model, electrical control model, mechanical control model and pitch control model. These models will be explained in the next chapters. Figure 31 shows a simple schematic of an individual wind turbine, and figure 32 shows the interaction between the modules.

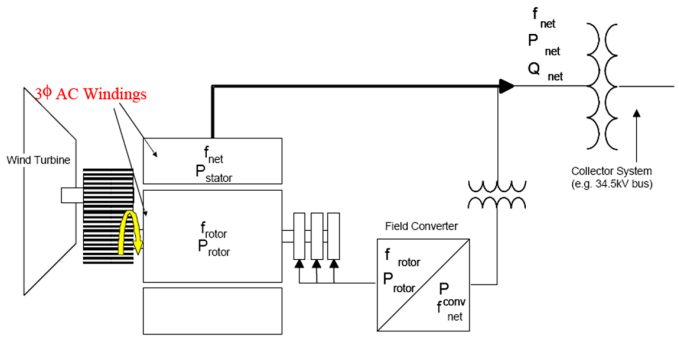

Figure 31: GE WTG major components [21]

10.1.1 Load flow model

Figure 33 shows the load flow model. The generator is connected to a PV bus at 4160 V. The generator terminal bus is connected to the collector system bus through a suitably rated transformer. Voltage level at the collector system is set to 33 kV, as explained in chapter 9.1. The transformer power rating is 4MVA with a 6% leakage reactance. Each GE 3.6 machine has a rated power output of 3.6 MW. The reactive power capability of

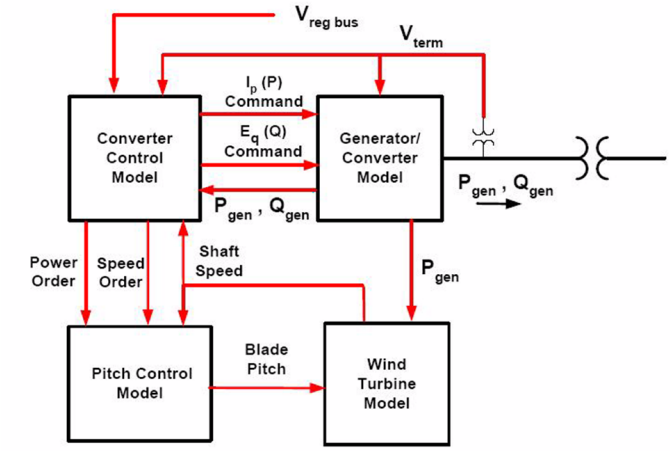

Figure 32: Interaction between the dynamical WT3 modules [24]

each machine is ±0.9 pf, which corresponds to Q_{max} ≈1.74 MWAr and Q_{min} ≈-1.74, and an MVA rating of 4.0 MVA. The minimum steady-state power output is 0.5 MW. The load flow inputdat and the PSS/E load flow data input can be found in appendix A.1.

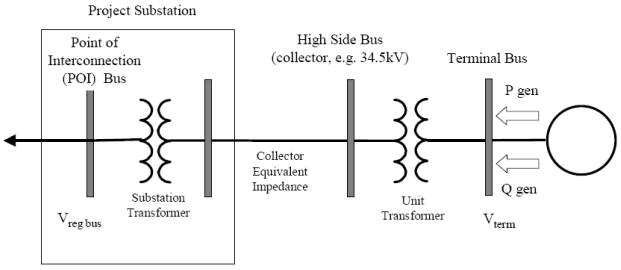

Figure 33: Load flow model of the GE WTG [21]

The generator can regulate the voltage at a bus by measure the voltage at a particular bus, and regulate this voltage by sending a reactive power command to all of the wind turbines. In load flow the wind turbine generators should be set to regulate the same remote bus, which is often the point of interconnection (POI) with the transmission system. The WTG was set to regulate the point of interconnection.

10.1.2 Generator/converter model

Figure 34 shows the generator/converter model. The output of the model is a controlled-current source that computes the required injected current into the network in response to the flux and active current commands from the excitation (converter) model. The converter control includes a phase-locked loop to synchronize the generator rotor currents with the stator. The function of the converter phase-locked loop is to establish a reference

frame for the WTG voltages and currents, that is shown in the phase diagram in figure 35. In steady-state $V_x = V_{term}$. In case a system disturbance, the rate of change is limited by the PLL logic. X_{eq} represents an equivalent reactance of the generator effective reactance.

The PSS/E dynamical input data for the generator/converter model are given in appendix A.2.

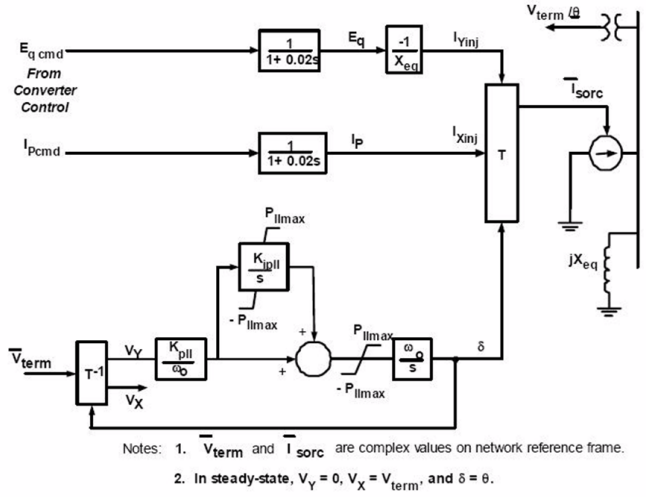

Figure 34: Generator/Converter model of the WT3 [24]

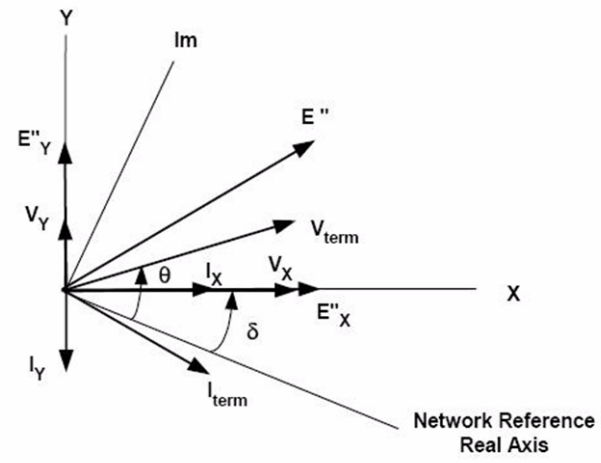

Figure 35: Phase diagram of the voltages and currents given in the generator/converter model of the WT3 [24]

10.1.3 Electrical converter model

Figure 36 shows the reactive power control model, and figure 37 shows the torque control model. In PSS/E are these two models are represented in one dynamical model, which is the electrical converter model.

If the varflag in the reactive power control model is set to 1, the terminal voltage at the voltage regulated bus (V_c) is compared against the reference voltage (V_{rfq}), to create the voltage error. This error is used to compute the Q_{cmd}. Another possibility is constant reactive power regulation. The varfalg is then set to 0. Q_{cmd} is then the given by the reactive power from the load flow.

If the vltflg was set to 1, the terminal voltage (V_{term}) is compared against the reference voltage (V_{ref}), to create the voltage error (V_{err}). This error is then multiplied by a gain and integrated to compute the voltage command E_{qcmd}. If the vltflg is set to 0, the integral of the error between Q_{cmd} and Q_{gen} is used directly to compute the voltage command E_{qcmd}.

In the load flow model, all the turbines was set to regulate the voltage at point of interconnection. This is done by sending a reactive power command to all of the wind turbines. In the AC/AC system, Varflag is therefore set to 1. In the AC/DC system, Varflg is set to 0, because the HVDC Light can control the reactive power.

Vltflag was set to 0. This was done because the wind turbines regulate the voltage at point of interconnection.

The torque control model computes the current command I_{pcmd} and controls the mechanical torque.

The PSS/E dynamical input data for the electrical converter model are given in appendix A.3.

10.1.4 Mechanical control model

The function of the wind turbine model is to extract as much power from the available wind as possible without exceeding the rating of the equipment. This model computes the turbine speed that influences the blade pitch and the generated power. Figure 38 shows the single mass mechanical system model, and figure 39 shows the two-mass mechanical system model. In a single mass mechanical system, the shaft is represented by a stiff shaft, and the inertia in the turbine and the generator can be represented by one total inertia constant. In a two-mass mechanical system, the shaft is represented by shafts, which can be twisted independently of on another within a certain limit. The input parameter F_{req1} determine the selection of mechanical model, which defines the first shaft torsional resonant frequency [Hz]. The two-mass mechanical system is used in the GE 3.6 WTG.

The PSS/E dynamical input data for the mechanical control model are given in appendix A.5.

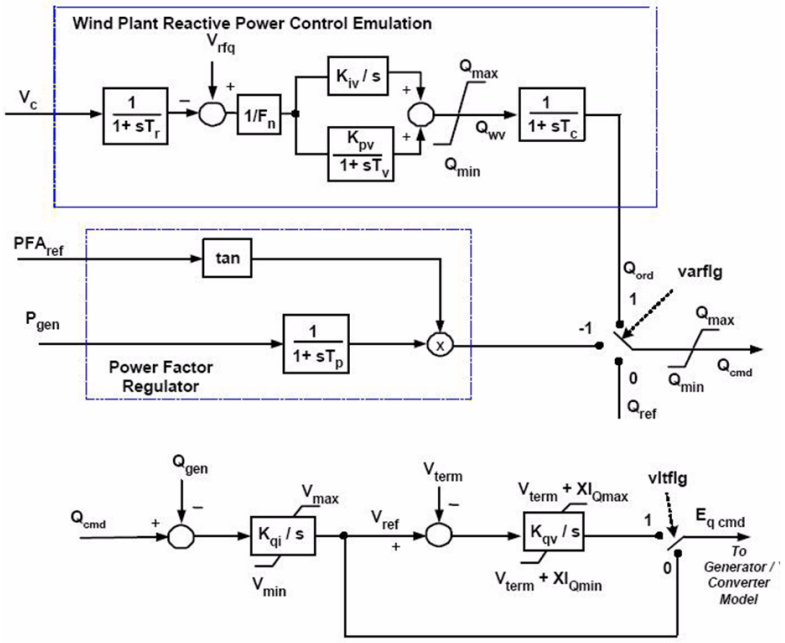

Figure 36: Reactive power control model of the WT3 [24]

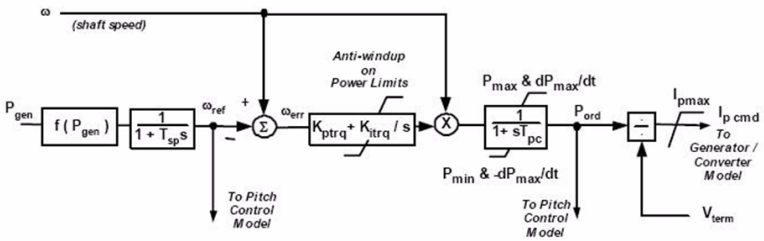

Figure 37: Reactive power control model of the WT3 [24]

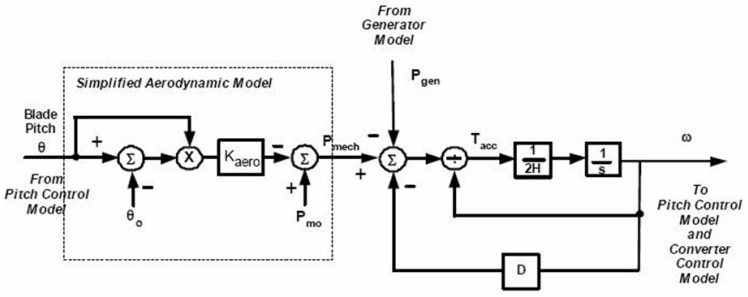

Figure 38: Single mass mechanical model of the WT3 [24]

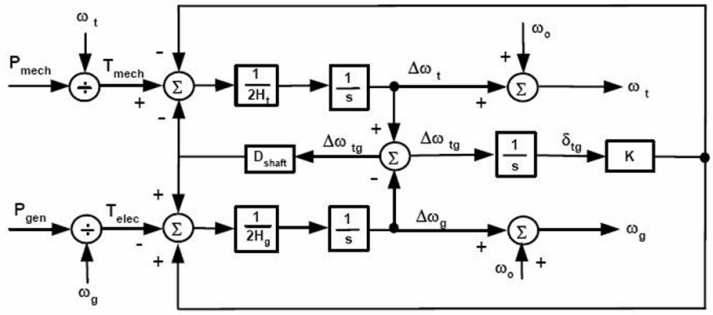

Figure 39: Two-mass mechanical model of the WT3 [24]

10.1.5 Pitch control model

Figure 40 shows the pitch model. The inputs to this model are the speed order ($\omega\ _ref$) and power (P_{set}) from the converter control model, shaft speed (ω) from the turbine model, and the generated power given by the load flow (P_{ord}). The output is blade pitch (θ), which is an input to the mechanical control model.

The PSS/E dynamical input data for the pitch control model is given in appendix A.5.

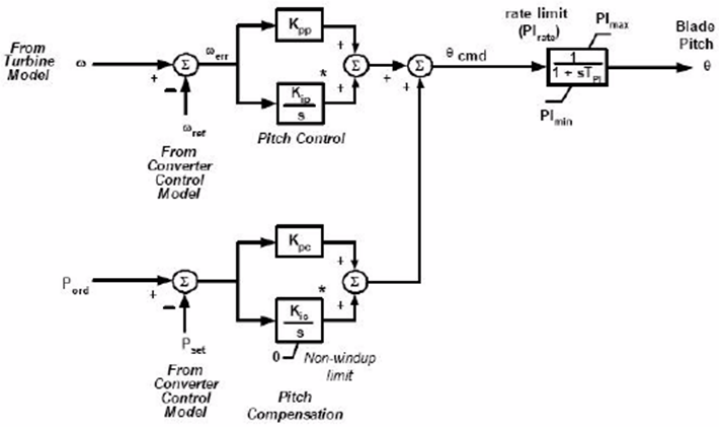

Figure 40: Pitch model of the WT3 [24]

10.2 Cables

The distance between each wind turbine was is six rotor diameters. With a rotor diameter of 104, the distance between each turbine is 0.624 km. Normally, the distance from seabed to the wind turbine is 100 m, and the cable length at seabed should include % slack of the distance at seabed [27]. The total distance between each turbine is therfore 0.8427 km. 3% slack is added because the cable does not necessarily follow a stright line. The cable between each wind turbine has three different conductor cross-sections. The calculated

resistance, inductance and shunt capacitance between each wind turbine are given table 3, based on the technical data given in chapter 9.5.

Table 3: Cable data for the cables between the wind turbines in each radial

Cross-section $[mm^2]$	Power rating $[MW]$	Resistance $[ohm]$	Inductance $[ohm]$	Shunt capacitance $[\mu F]$
120	18.6	0.16854	0.10857	0.15169
240	29.3	0.08427	0.09796	0.19383
400	36.4	0.05056	0.09266	0.23596

The cable length from the first wind turbine, counted from the offshore platform, to the offshore platform varies from radial to radial. Cables on the opposite side of the radial in the middle, have the same cable length to the platform. Instead of calculate the cable data for each radial, the radials was divided in three groups with three different cable lengths. The length from the platform to the ten radials in the middle, was set to 2 km. The length to the next six radials, was set to 7 km. the last six cables, was set to 12 km. The calculated resistance, inductance and shunt capacitance of the cable from the offshore platform to the radials are given in table 4. Total cable length includes 100 m from seabed to wind turbine and platform, and 3% slack is added to the cable at seabed. String 1 is the first radial to the left in the configuration, seen from offshore to shore.

Table 4: Cable data for the cables between the offshore platform and the radials

String	Total cable length $[km]$	Resistance $[ohm]$	Inductance $[ohm]$	Shunt capacitance $[\mu F]$
1-6 and 29-34	12.56	0.7536	1.38104	3.5168
7-12 and 23-28	7.41	0.446	0.81477	2.0748
13-17 and 18-22	2.26	0.1356	0.24845	0.6328

10.3 Equivalent

As explained in chapter 9.6 some strings are modeled with one wind turbine, one transformer, and all the cables between the wind turbines are lumped together in one cable to the offshore platform. This chapter explains how the equivalent is modeled.

10.3.1 Wind turbine

The eight wind turbines in one radial are modeled as one wind turbine. The rated power output is multiplied by eighth. This corresponds to an MVA rating of 32 MVA. The reactance was set to the same value as for one wind turbine. In the dynamical model it is possible to choose how many wind turbines one modeled wind turbine represents. The equivalent turbine was therefore set to represent eight wind turbines.

The load flow inputdat and the PSS/E load flow data input can be found in appendix A.6.

10.3.2 Transformer

The transformer equivalent is modeled as the wind turbine equivalent. Each individual transformer has a power rating of 4 MVA. The power rating of each transformer equivalent is then 32 MVA. The reactance was set to the same value as for one transformer.

The load flow input data and the PSS/E load flow data input can be found in appendix A.6.

10.3.3 Cables

The cables between each wind turbine are modeled as one cable and summarized with the cable to the offshore platform. In this study, the equivalent impedance was calculated by taking the average of the three different impedances used for the cables between the wind turbines. The calculated equivalent impedance is given in table 5. The calculated impedance of the cable to the offshore platform, is given table 6. The cable data for the equivalent impedance is multiplied with the total cable length between seven wind turbines and summarized with the cable data for the cable to the offshore platform.

Table 5: Cable data for the equivalent cable between the wind turbines in each radial

Cross-section $[mm^2]$	Power rating $[MW]$	Resistance $[ohm]$	Inductance $[ohm]$	Shunt capacitance $[\mu F]$
120	18.6	0.2	0.1288	0.18
240	29.3	0.1	0.11624	0.23
400	36.4	0.06	0.10996	0.28
X_{eq}		0.12	0.11833	0.23

Table 6: Cable data for the cables between the offshore platform and the radials

String	Resistance $[ohm]$	Inductance $[ohm]$	Shunt capacitance $[\mu F]$
1-6 and 29-34	1.51859	2.13540	4.9830
7-12 and 23-28	1.20959	1.56913	3.54103

10.4 Transformers

The transformers at the offshore platform are modeled as one transformer. Voltage level for the transformer in the AC/AC system is 33/420 kV. At shore the voltage level is 300/420 kV, because the voltage level at the swing bus are set to 300 kV.

The HVDC Light converters are connected to transformer with voltage level at 400/416 kV. This transformer is connected in series with the other transformer. The voltage level is corrected in proportion to the HVDC Light transformer.

Load flow input data for the transformers was given by [28]. These are given in the table 7. All transformers, except the HVDC Light transformers, were modeled with the same technical data.

Table 7: Individual WTG load flow data

E_k=Z %	17%
E_r=R	0.0035 pu
X	0.169964 pu

where X are given by

$$X = \sqrt{Z^2 - R^2} \tag{14}$$

The PSS/E load flow data input can be found in appendix A.9

10.5 HVDC Light

ABB has made user model of HVDC Light for simulation in PSS/E. This chapter will explain the use of the model in PSS/E. A user manual is provided, with information for PSS/E implementation [2]. Technical data for this model can not be listed, since this is confidential information.

10.5.1 Load flow model

Figure 41 shows the load flow model of the HVDC Light system. The two generators represents the converters, and regulates the voltage at the bus PCC. The ac filters are represented by the reactive power generation of the ac filter capacitors. The buses named PCC are the point of connection to the ac system.

The main data are given in the model, but the user must specify the active power at each converter, but only the power level of the inverter are specified in PSS/E. This is because the bus which the rectifier are connected to, are set to be a swing bus. The power level of the inverter must me positive and the power level of the rectifier must be negative. Power level of the inverter must be selected in such a way that a realistic level of losses is attained. The user must also select a combination of active and reactive power that is within the PQ diagram in figure 42. Calculation of losses are explained in chapter 10.5.2.

In this thesis, the converter type M9 is used because this is the only converter type that has a suitable power rating. Technical data for the different converter types are given in [1]. The power rating of the converter type M9 is 1216 MWA.

10.5.2 Losses

The DC cables are not modeled in the load flow. As mentioned in the previous chapter 10.5.1 the user must select the power level of the inverter in such a way that a realistic level of losses is attained. Power losses in the DC system is given by

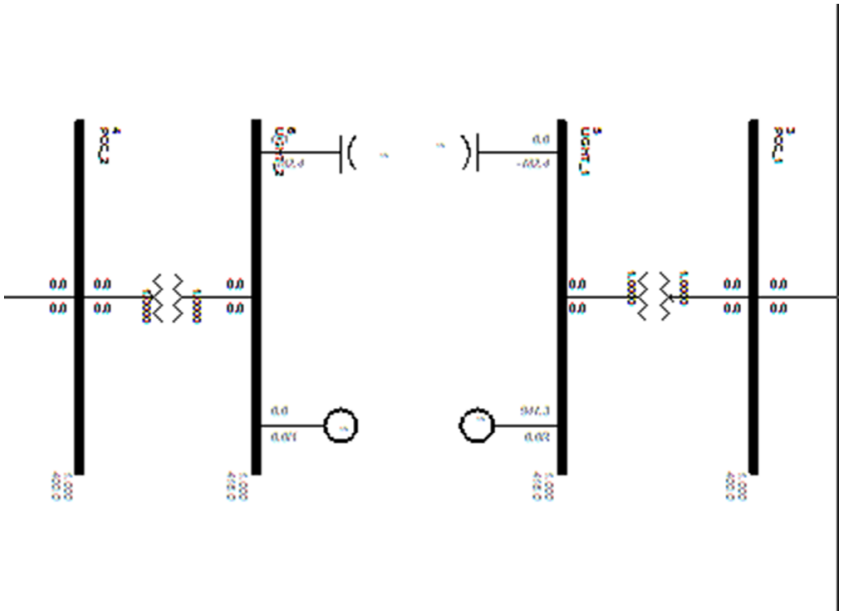

Figure 41: Load flow model of the HVDC Light system

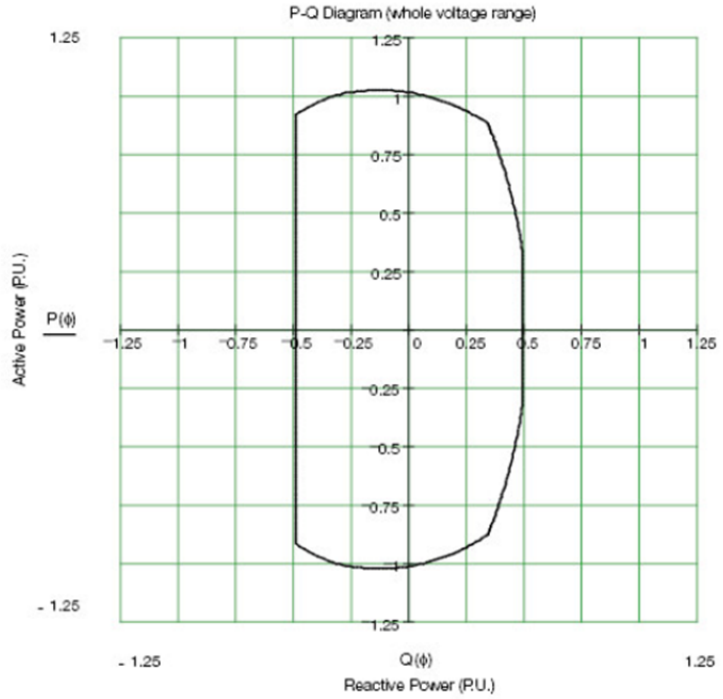

Figure 42: PQ-diagram [1]

$$P_{loss} = -P_{rectifier} - P_{inverter} \tag{15}$$

where P_{loss} consists of converter and cable losses. The converter losses are 20.15 MW in each converter at full power. It is assumed that the converter MW losses are independent of the power transferred, since most of the losses are caused by the switching of the IGBT´s [26].

The cable losses are calculated by finding the DC current, which is given by

$$I_{dc} = -P_{rectifier/sending}/V_{dc} = 978.963 \bullet 10^6/320 \bullet 10^3 = 1498,14A \tag{16}$$

$$P_{cableloss} = 2 \times R_{cable[ohm/km]} \times length \times I_d^2 = 2 \times 0.79 \times 77,65 \times 1498,14^2 = 2,7534MW \tag{17}$$

where the cable resistance are taken from [2], and the total cable length includes the distance from platform to seabed and 3% slack of the cable length at seabed. The sending power are calculated in the load flow simulation, which is explained in chapter 11.1.2. From this the power level of the inverter can be calculated.

$$P_{inverter} = P_{rectifier} - P_{loss,converters} - P_{loss,cable} = 979 - 40.3 - 2.75 = 935.95 \tag{18}$$

If the load flow losses does not match the dynamic losses in the initialization,and the difference is large, a warning message with the mismatch is written in the PSS/E output window. The difference between the initial dynamic losses and the load flow losses is adjusted with the parameter PlossAdjust, and is kept constant during the dynamic simulation. In this case the mismatch was 2.72 MW. The recieving power was instead increased to 941.267 MW.

From the PQ diagram the reactive power level of the ac filters are specified. The power level are given in table 8.

Table 8: Reactive power level of the ac filters

	$Q_{max}\,[MW]$	$Q_{min}\,[MW]$
Filter rectifier	425	-608
Filter inverter	486	-608

10.5.3 Dynamical model

A PSS/E user model has been developed to represent the function of an HVDC Light transmission, CABBL2, which represents the converters. The user model CABBL2 is used to calculate the current injection to be applied by the generators modeled in the load flow. The interacting between the dynamical model and the representation in the load flow is shown in figure 43.

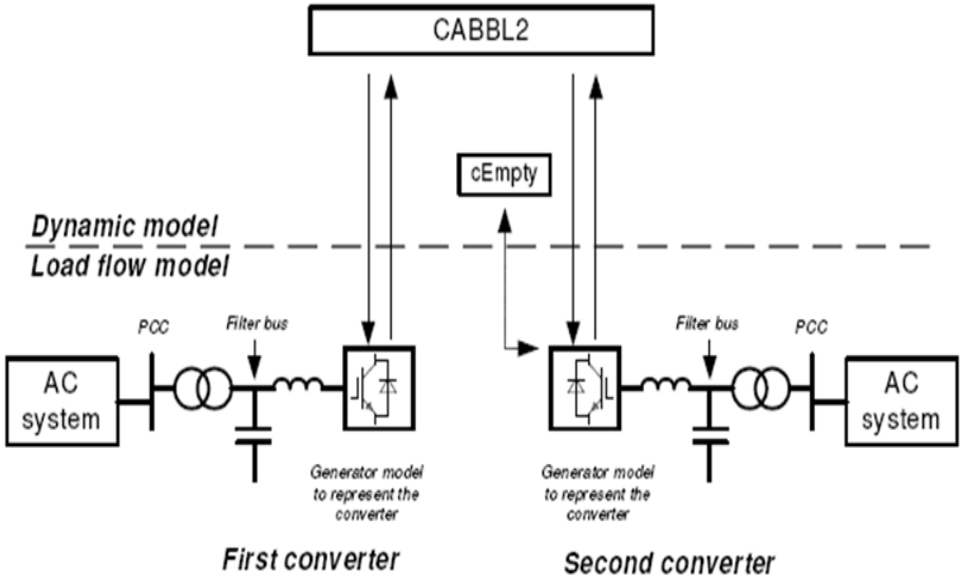

Figure 43: Overview of the interaction between the load flow and dynamical model [2]

The control principle for a HVDC Light converter in an offshore wind farm ac system, are different from a converter connected in a large transmission system. The passive net operation mode for an offshore wind farm application use frequency and voltage control. In wind farm application, the CtrlParamAlt should be 2. In the DLL user model files, it is not possible to change this parameter. Therefore the converters act as a slack bus balancing the load in the system during the restoration process of ac system.

During simulations there is a risk for numerical oscillations. A user parameter U_{ac} and Q control gain reduction, UacQGainRed. Using the gain gain reduction remove these oscillations. The parameter is to be used at weak systems. Also this parameter is not possible to be change.

10.6 Static Var Compensation

In PSS/E there are several dynamical models that represent an SVC. The model that is used in this study is CSVGN5. Figure 44 shows the Static var Compensation model. Based on the voltage at the selected voltage regulated bus, this model regulates the reactive power delivered or absorbed from the network. In load flow this model is represented with a generator. The load flow and dynamical input data are given in appendix A.8. The power rating of the SVC is based on simulations explained in chapter 11.1.1. The selected dynamical data gives a very conservative responds after a fault.

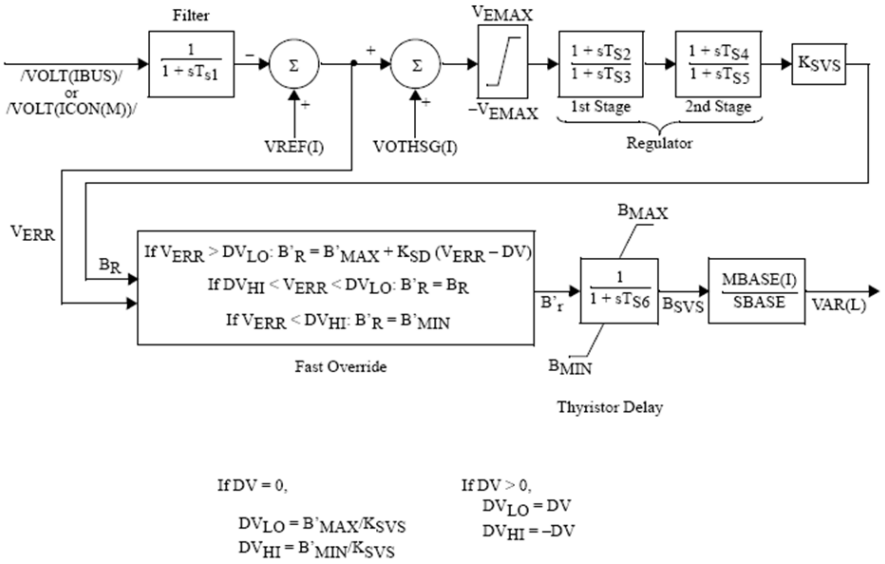

Figure 44: SVC model [24]

10.7 Swing machine

In load flow the swing machine is modeled as a generator with no limitation of reactive and active power. The dynamical model is called GENCLS. The PSS/E dynamical input data for the GENCLS model is given in appendix A.10.

11 Case study

Before a dynamical simulation can be done, a load flow case has to be established for the two configurations. This chapter will first present the load flow results. To investigate the transient stability in the two systems, two disturbances are applied to the systems. The systems are studied at full power production.

11.1 Load flow

This chapter presents the load flow results. In order to fulfill the requirements regarding reactive power control at the connection point, an SVC had to be added in the AC/AC system.

11.1.1 AC/AC configuration

The system was first tested without an SVC. The first test was done with power production of 3.6 MW. In appendix B.1 the generator VAR limit checking report can be found. The generators that are listed are generators that exceeds the VAR limits. The generator VAR limit checking report shows that the all the generators except the equivalents exceeds the reactive power limit. The reason why the generators exceed the limit of reactive power is because the generators are set to regulate the voltage at the high voltage side if the transformator. To obtain the wanted voltage the generators absorbs the reactive power produced in the transmission cables to shore. With reactive power compensating this problem can be solved.

SVC was put on shore because the generators are set to regulate the high voltage side of the offshore transformer. To find a suitable SVC the power production was set to 0.5 MW, because the system has to be able to operate within given required limits in the whole range of power production. At low power generation the reactive power production in the cables are higher, so the worst case is minimum power output.

Test with SVC of 100 MVA gave too high voltages. The busbar voltage limit checking report is found in appendix B.2. The voltages are too high at the high voltage side of offshore transformer and at the connection point at shore. But the generators reactive power production did not exceed the limits. The SVC MVA limit was increased until the voltages became within acceptable limits, and until the power factor at the swing bus became $\pm$ 0.95. Acceptable limit of the voltage is described in chapter 5.1.

An SVC of 570 MVA gave a solution within acceptable limits. Appendix B.3 and B.5 shows the load flow result for power production of 0.5 MW and 3.6 MW. When the power production is 3.6 MW the SVC absorbs only 234.1 MVA.

Appendix B.4 and B.6 shows the busbar voltage limit checking report for power production of 0.5 MW and 3.6 MW. At power production 0.5 MW the voltage are lower than 0.9 pu at the buses that the equivalent wind turbines are connected to. At power production of 3.6 the voltage are lower than 0.9 at all the generator terminal buses. Since voltage is not lower than 0.87 pu no action is needed.

At full power production the cable from the radials to the offshore transformer, the offshore transformer, and the transmission cables are overloaded. Table 9 shows the selected power ratings and the required power ratings.

Table 9: Required power rating

Equipment	Power rating [MVA]	Required power rating [MVA]
Cable to platform	36.4	37
Offshore transformer	1200	1300
Transmission cables	550	650

11.1.2 AC/DC configuration

The AC/DC system does not need any reactive power compensating. The load flow results is found in appendixB.7, and the busbar limit checking report is found in appendixB.6. The wind turbines are now producing some reactive power in order to regulate the voltage at the high voltage side of the transformer. The converters absorb reactive power produced by the ac filter. The voltages are higher than 1.05 pu at the generator terminal buses.

11.1.3 Losses in the two systems

The results from the load flow shows that the losses are higher in the AC/DC system. The losses in each systems, based on the power delivered to the network, is found in table 10. The losses in the AC/DC system are 5.8 % higher than in the AC/AC system.

Table 10: Required power rating

System	Power generation [MW]	Power delivered [MW]	Losses [MW]
AC/AC	1008	942.5	65.5
AC/DC	1008	938.7	69.3

11.2 Event 1

In event 1, a fault at the swing bus is applied, with shunt impedance to ground larger than zero. In PSS/E, shunt resistance and reactance are given in MW and MVA power for the actual voltage at the busbar. In this event, a power of -2E+009 MVAr were added to simulate the fault. The same power was added in event 2. The shunt reactance are given by

$$X_{shunt} = \frac{U_{ac}^2}{Q} = \frac{(300 \times 10^3)}{-2 \times 10^{9+4}} = -0.0045 ohm \tag{19}$$

The bus fault was removed after 100 ms. This fault is suppose to represent a three-phase fault at one of the lines connected to the connection point. The line is disconnected after 100 ms.

11.2.1 AC/AC configuration

Figure 45 shows the plot of the voltage at the swing bus. The voltage at the swing bus is reduced to zero during the fault. Figure 46 shows the plot of the voltage at the high voltage side of the offshore transformer (HSP-offshore) and at a generator terminal bus, compared with with the voltage at the swing bus. The plot shows that the voltage at the HSP offshore bus and the generator terminal bus is also reduced during the fault, but it is not zero. This is because the generators produce reactive power during the fault to increase the voltages. The voltage at the swing bus are recovered after approximately 4 seconds after the fault.

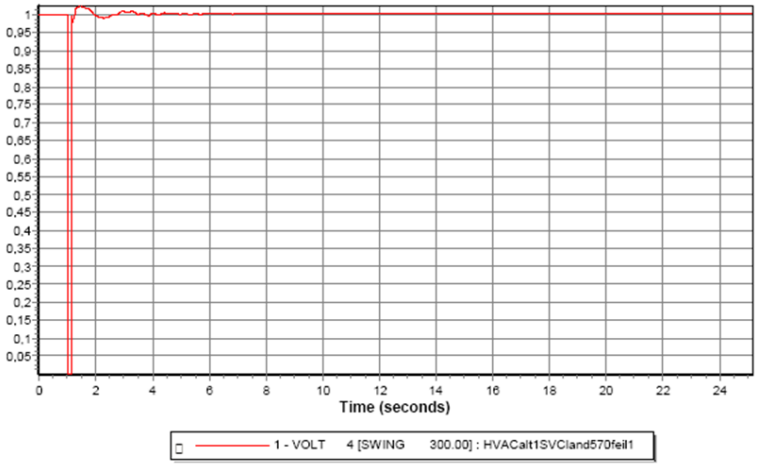

Figure 45: Voltage at swing bus

Figure 47 shows the plot of the reactive power flow between the connection point at shore and the swing bus, and between offshore and the connection point at shore. The plot of the reactive power transfer between the connection point at shore and the swing bus, shows how the SVC responds during and after the fault. When the fault occurs, the reactive power absorbed by the SVC can not change immediately because of the coils that absorbs reactive power,so the SVC absorbs the same amount of reactive power as before the the fault. After the fault the SVC regulates the reactive power in order to maintain the voltage at shore at approximately 1 pu.

Figure 48 shows how the reactive power from the generator are regulated by the voltage at the HSP-offshore bus. When the voltage increase the generator increase the absorbation of reactive power and vice versa.

Figure 49 shows that the speed of the wind turbines increase during the fault because of the reduced electrical torque caused by the fault. The turbine is pitched to reduce

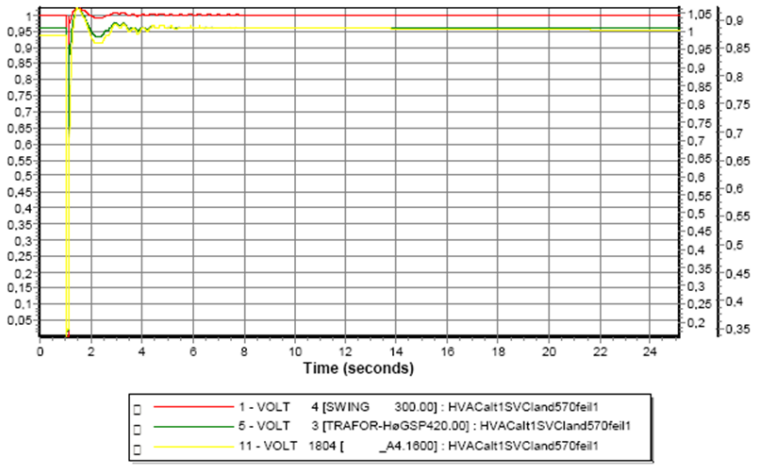

Figure 46: Voltage comparison of the voltage at the swing bus, HSP-offshore bus, and at a generator terminal bus

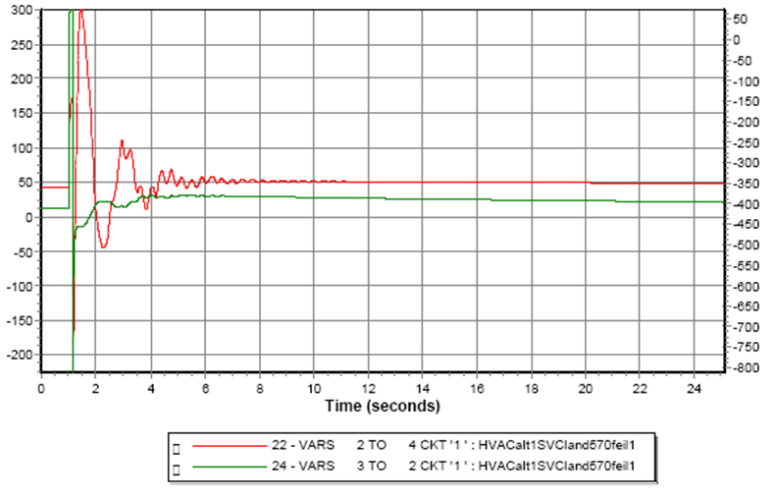

Figure 47: Reactive power flow between the connection point at shore and the swing bus, and between offshore and shore

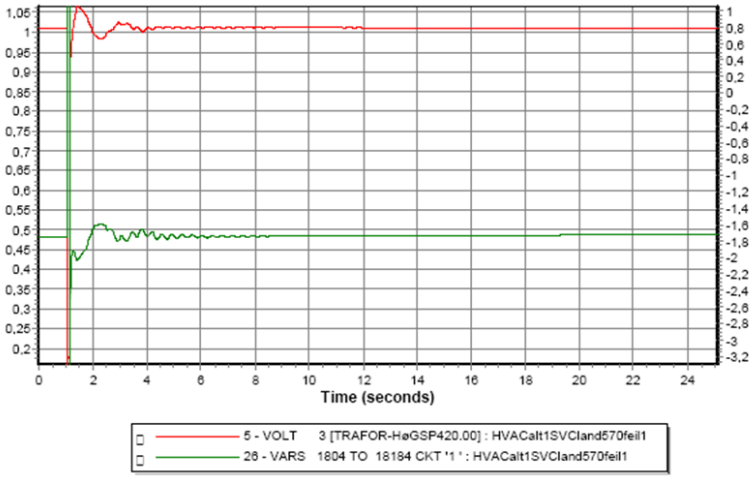

Figure 48: Voltage at the HSP-offshore bus, and the reactive power from the generator

the speed. When the power output after the fault is lower than the power from the load flow, the turbines are pitched to increase the power output. This can be seen from the power output curve in the same figure.

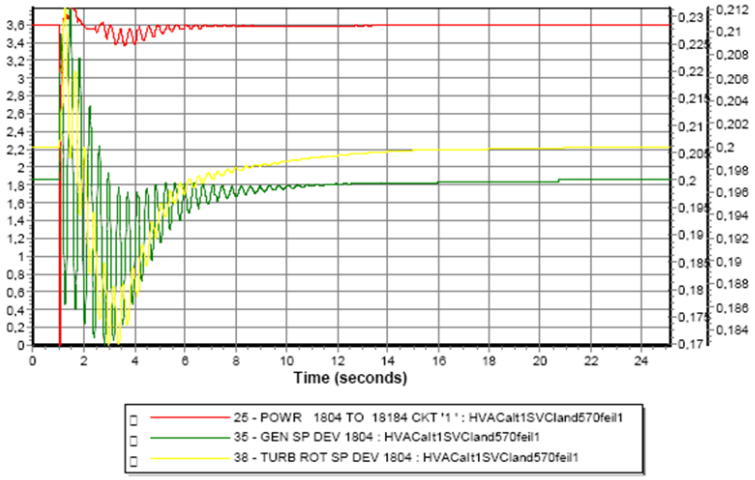

Figure 49: Generator speed deviation and turbine rotor speed deviation, and generated power by one generator

Figure 50 shows the plot of the generator speed deviation for a generator, compared with an equivalent generator. The figure shows that the equivalent generator behaves as the other generators.

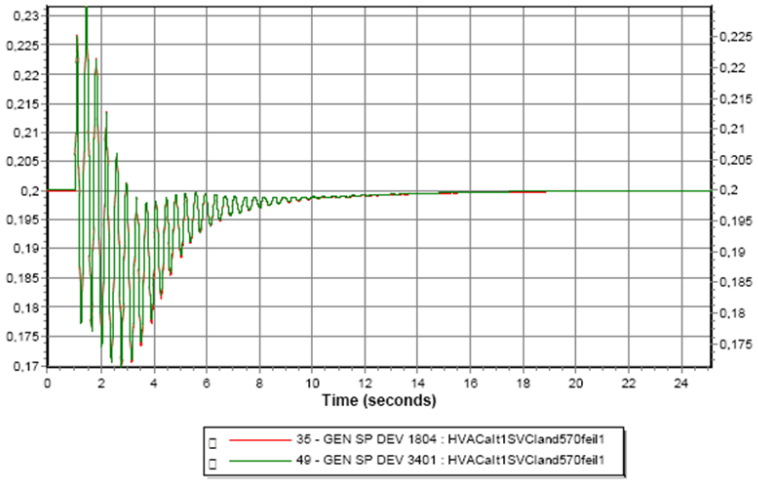

Figure 50: Generator speed deviation for a generator, compared with a equivalent generator

11.2.2 AC/DC configuration

Figure 51 shows the plot of the voltage at the swing bus. The figure shows that the voltage is decreased to zero during the fault. The voltage is recovered after approximately 0.5 second after the fault. Figure 52 shows the voltage at the swing bus, and at the converter bus at shore. The figure shows that the voltage at the converter bus is reduced during the fault, but it is not decreased to zero. This is because of the reactive power delivered from the converters.

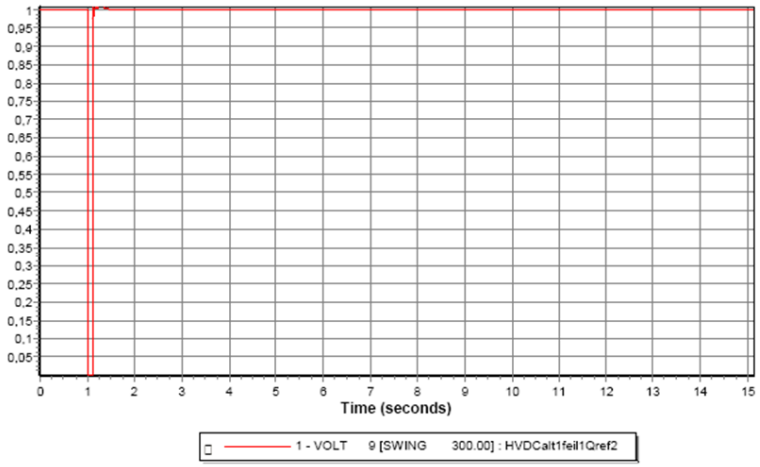

Figure 51: Voltage at the swing bus

Figure 53 shows the plot of the reactive power flow between the connection point

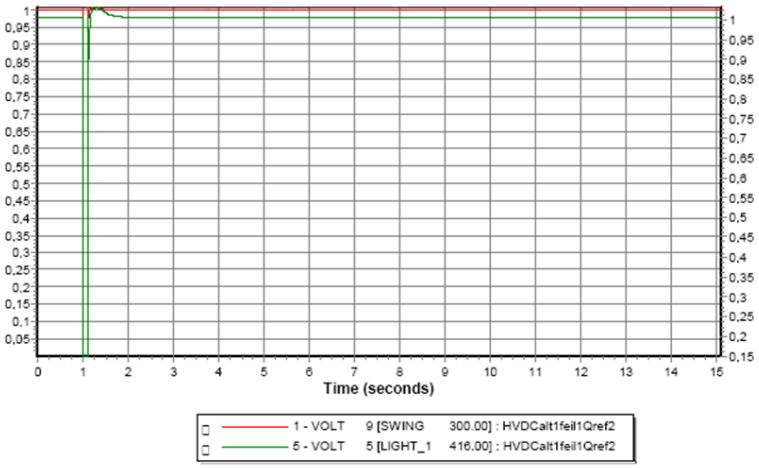

Figure 52: Voltage at swing bus and converter bus at shore

at shore and the swing bus. During the fault, reactive power is delivered from the converter at shore. Right after the fault the reactive power increase rapidly and decrease to approximately 60 MVA. Right after the fault the the reactive power decrease rapidly to -1000 MVA. This is because of the numerical oscillations as explained in chapter 10.5.3.

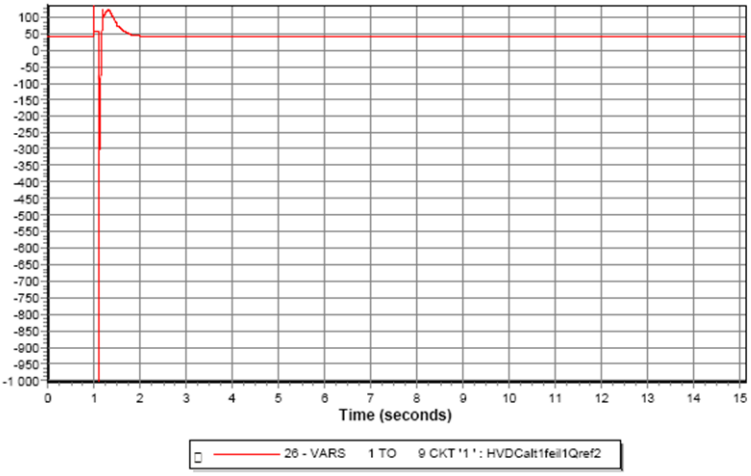

Figure 53: Voltage at swing bus and converter bus at shore

Figure 54 shows how the reactive power delivered by the generator is regulated. In this system this is done by constant reactive power regulation. Therefore are the oscillations of the reactive power and also of the voltages more constant. The reason why the reactive power and the voltage increase after the fault is because the converter at shore block when the fault occurs.

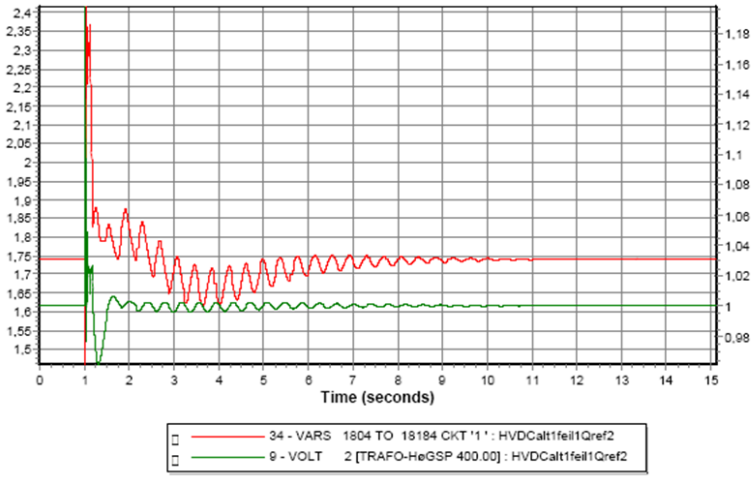

Figure 54: Reactive power delivered by generator at bus 1804 and the voltage at the HSP offshore bus

11.2.3 Comparison of voltage at connection point at shore

Figure 55 shows the plot of the voltage at the connection point at shore in the AC/AC and the AC/DC system. The voltage at shore in the AC/AC system is a bit higher during fault than in the AC/DC system. This indicates that the AC/AC system has a higher short-circuit MVA than the AC/DC system.

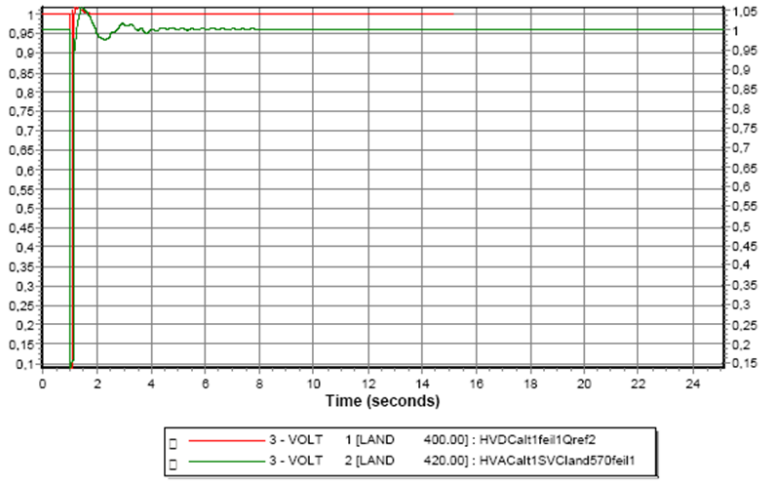

Figure 55: Voltage at connection point at shore in AC/AC and AC/DC system

11.3 Event 2

In event 2, a fault is applied at the bus that all the wind radials are connected to, with shunt reactance to ground larger than zero. The bus fault was removed after 100 ms. This fault is suppose to represent a three-phase fault near the connection point at on of the cable to the offshore transformer. After 100 ms the fault is cleared and the cable is disconnected. The line that is tripped is the cable from string 21, counted from left and seen from the offshore side.

11.3.1 AC/AC configuration

Figure 56 shows the plot of the the voltage at the low voltage side of the offshore transformer. The voltage is reduced to zero during the fault. Figure 57 shows the plot of the voltage at the HSP-offshore bus and at one of the generator terminal buses. The voltages are reduced during the fault, but because of the reactive power delivered from shore and from the generators, the voltage are not zero. The voltage at the HSP-transformer bus during the fault, depends on the short-circuit MVA of the AC system that the wind famr is connected to. Figure 59 shows the plot of the reactive power flow from offshore to shore, and from shore to the swing bus.

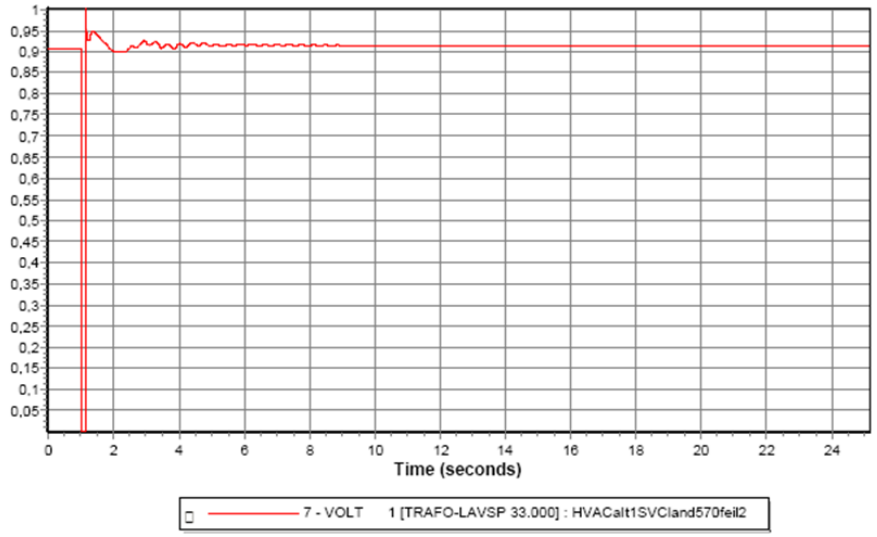

Figure 56: Voltage at the low voltage side of the offshore transformer

Since one of the radials are disconnected, the active and reactive power generation are different after the fault. This can be seen from the plot in figure 58 and figure 59. After the fault, the delivered power from the wind farm is reduced with 28.8 MW. The reactive power that was absorbed by the generators in the disconnected string, are now absorbed by the SVC.

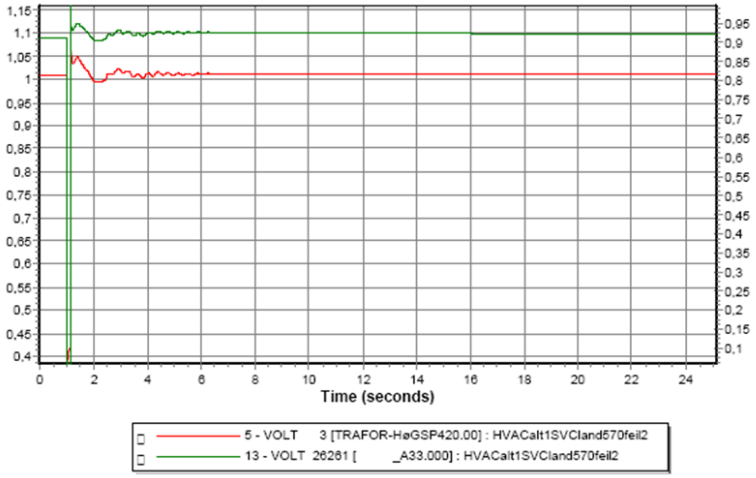

Figure 57: Voltage at the HSP-offshore bus and at one generator terminal bus

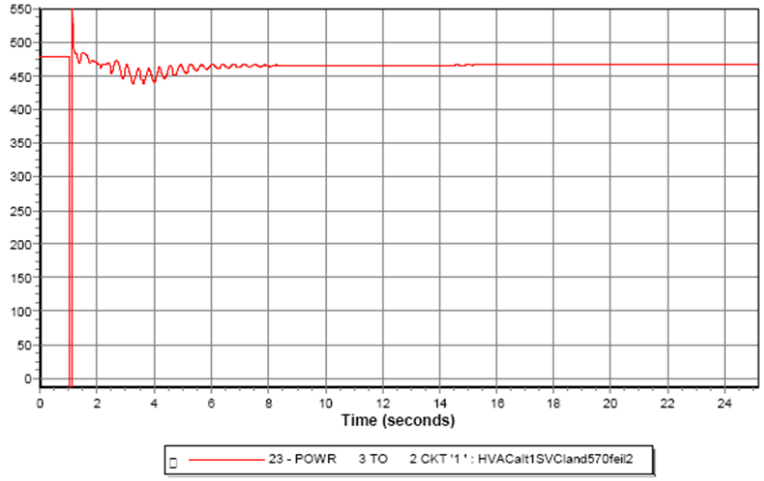

Figure 58: Active power generated by the wind farm

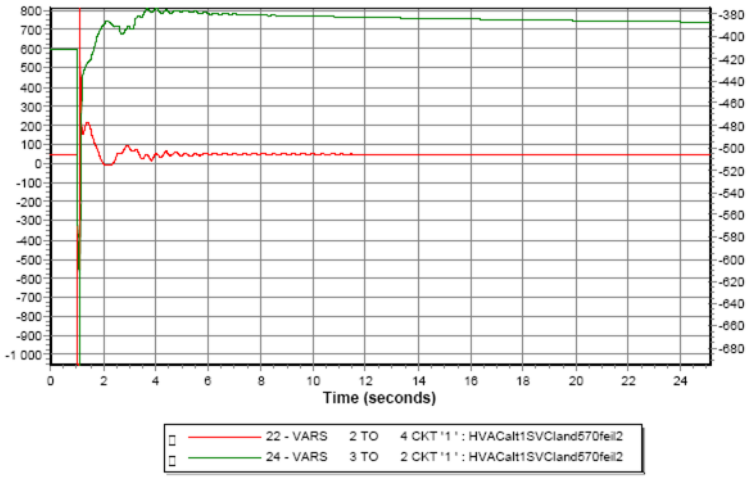

Figure 59: Increase in reactive power absorption by the SVC

11.3.2 AC/DC configuration

Figure 60 shows the plot of the voltage at the low voltage side of the offshore transformer. The fault is reduced to zero. The plot of the voltage at the high voltage side of the offshore transformer are shown in figure 61. Compared with the voltage at the same bus in the AC/AC system, is the voltage lower in the AC/DC system. This is because the reactive power delivered by the HVDC Light is than the reactive power delivered by the AC system. The plot of the reactive power flow between the point of connection of the HVDC Light and the converter bus offshore, is shown in figure 63.

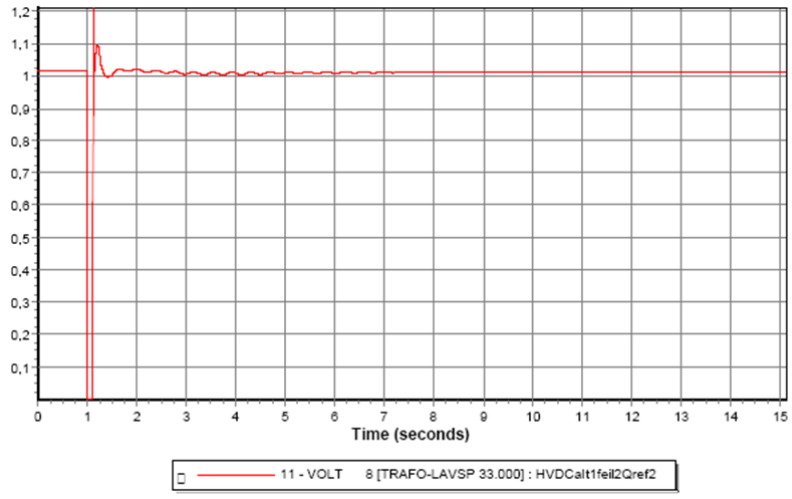

Figure 60: Voltage at the low voltage side of the offshore transformer

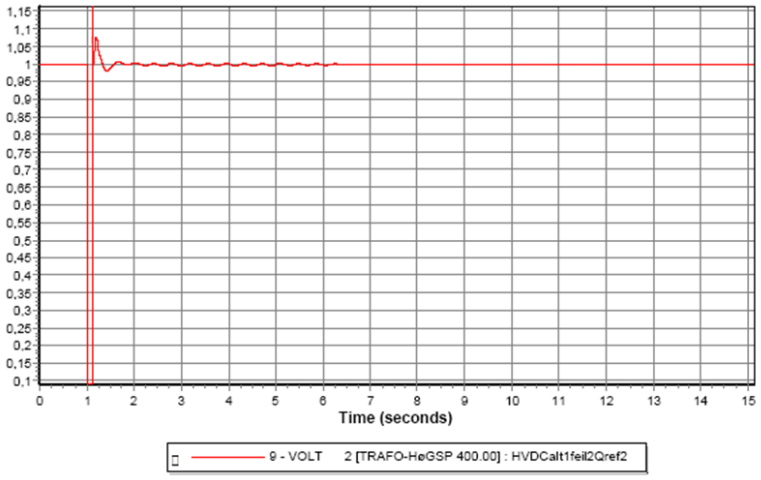

Figure 61: Voltage at the high voltage side of the offshore transformer

After the fault is cleared by disconnecting the cable, the active power generated by the wind farm changed. This does not happen in this case. The reason is because the HVDC Light converters act as a constant load, as explained in chapter 10.5.3. In order to keep the frequency at 50 Hz the generators have to compensate for the loss in generation. The reason of the high generation right after the fault is because of the numerical oscillations. This can be seen from the plot in figure 62. Figure 63 shows that the reactive power after the fault has changed. This is because the generators are set to regulate the voltage at the HSP-offshore bus by constant Q regulation, so the generators produce the same amount of reactive power as before the fault.

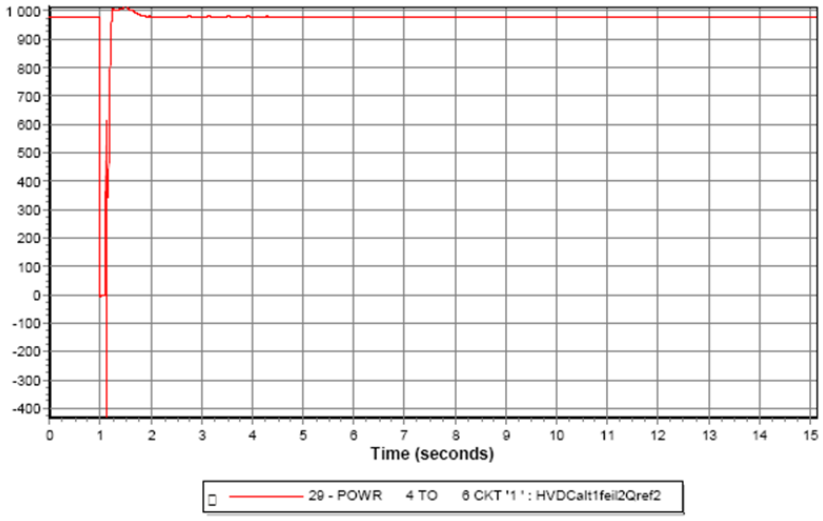

Figure 62: Active power generated by the wind farm

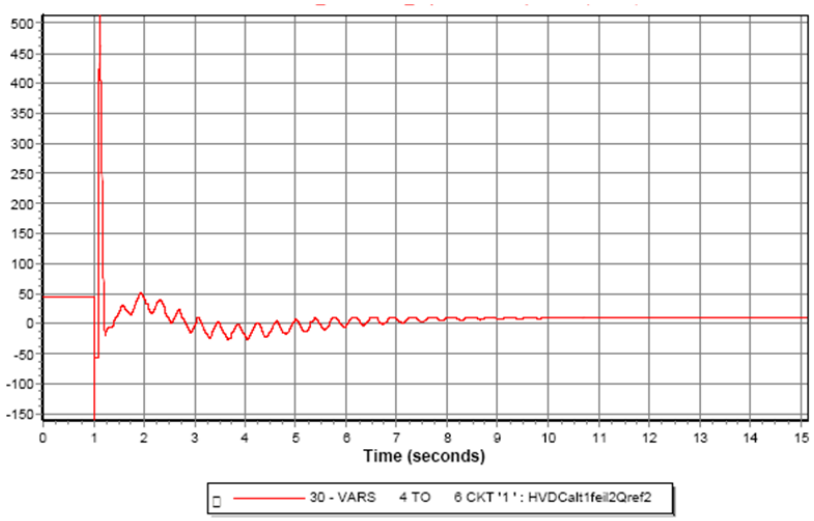

Figure 63: Reactive power flow between the point of connection of the HVDC Light and the converter bus offshore

12 Discussion

Certain aspects of the selection of technology are discussed consecutively in the previous chapters. An overall discussion of the selection of technology is made in this chapter as a summery.

According to the survey of different wind generator system and considering the grid connection requirements on wind turbines, the developing trends of wind turbine generator systems shows that variable speed is very attractive and concepts with full-scale power converters will become more attractive. Variable speed operation is very attractive because it reduces mechanical stress and increase power capture. Wind turbines with full-scale power converters may be more effective and less complicated to deal with grid related problems. Direct-drive concept with full-scale power converters has a higher overall efficiency, and the reliability and availability are also higher because of omitting the gearbox. Concepts with full-scale power converters are more expensive but the cost is decreasing. However, the multiple-stage geared drive DFIG concept with a partial-scale power converter is still the dominant concept in the current market.

The size of the wind farms has led to a problem of finding a suitable grid connection, which is strong enough to take care of the power from the wind farms. This and that the wind speed is more stable at the sea, leads to that in many cases the distance between the grid connection point and the wind farm is long. Over long transmission distances the losses in DC transmission are lower than in conventional AC transmission, and may therefore become more favorable. VSC HVDC has the ability to control both active and reactive power output. The converters are also self-commutating. This makes this system suitable for weak networks.

Blade geometry, pitch angle, rotor speed and so on will affect the wake effect. To avoid this, the wind farm can be made longer and more stretched out instead of quadratic. Radial, star and ring layout are three possible configurations of a wind farm. The slight of improvement in reliability with ring layout compared with the radial layout, will not even out the added cable costs.

To compete with other forms of power generation, wind power has to be cost-effective. The system has to be efficient in order to deliver as much power as possible. Efficient technology is more expensive, but will probably be more cost-efficient in a long term. At the sea the weather conditions are more demanding. This requires more robust wind turbines. These wind turbines may not be the most efficient, but maintenance offshore are more expensive and time consuming. Maintenance leads to loss in generation and income. To avoid loss in generation the system can be made more reliable. This will decrease the availability costs but increase the investments cost.

In this thesis two configurations of a 1000 MW offshore wind farm have been studied. Distance to shore is 75 km. The configuration of the wind farm was based on the radial layout with 35 strings, with eight wind turbines in each string. The difference between the two configurations is the transmission system. One system with AC/AC transmission and the other with AC/DC transmission based on the HVDC Light system. The two configurations were modeled in PSS/E.

The load flow results shows that the losses are 5.8% higher in the AC/DC system. If the distance to shore were increased the losses would have been lower in the dc system. The technical data for the ac cable to shore may also be wrong.

Two disturbances were applied to the systems. The dynamical result shows that both of the systems were stable. The results indicates that the short-circuit MVA is higher in the ac system than in the dc system. After a fault the voltage recovery was more smoother in the dc system, and the voltage recovery time were shorter.

In the electrical converter model of the wind turbine model that was used, it was possible to select the reactive power control. The reactive power in the ac system was controlled by the voltage at the high voltage side of the offshore transformer. In the dc system the reactive power were controlled by constant Q regulation based on the reactive power from the load flow. This was done because the HVDC Light can produce or absorb reactive power. The oscillations after a fault was more constant with constant Q control and the amplitudes were smaller.

It was also possible to control the voltage at the generator terminal buses in the electrical converter model. In case the voltages at the terminal buses are to high or to low this control can be used.

In the HVDC Light model that was used, there were some parameters that should have been changed. This was not possible. In the dynamical simulation this caused numerical oscillations. The second fault that was simulated, one of the strings in the wind farm was disconnected. This led to that the other generator produced more active power. The reason was that the HVDC Light model acts like a constant load because the model was in active power control mode, and not voltage and frequency mode. The mode could have been changed with the parameters that were not possible to change.

Today several plans on 1000 MW offshore wind farms exists. The size of the wind farms has led to a challenge of how to find an efficient and secure design of the overall system. The system has to be cost-effective in order to compete with other forms of power generation. An optimal configuration of an wind farm is a compromise between cost, robust and reliable system, and a efficient system.

In this study, costs have not been taken into concern, so which configuration is most cost effective is difficult to say. HVDC Light converters are expensive, but in the ac system it is necessary with an SVC of 570 MVA. Based on the assumption that has been made, the losses are higher in the dc system. The result shows that both of the selected configurations are stable, and fulfill the grid code connection requirements.

This thesis was written in cooperation with Statkraft. Statkraft will continue to offer students the possibility to write their master thesis in cooperation with them. An interesting case would be to do an economic evaluation of the investigated configurations in this thesis. Improvements based on the economic evaluation can be tested in PSS/E.

Another case could be to look at other configurations with use of other wind turbine concepts and wind farm layouts.

A model of Siemens's VSC HVDC Light technology HVDC PLUS is also available in PSS/E. Simulations with HVDC Plus can be done in order to compare this technology with HVDC Light.

References

[1] ABB. *It's time to connect*, 2008.

[2] ABB. *User guide for the PSS/E implementation of the HVDC Light Detailed model Version 1.1.7*, 2009.

[3] Lia Teledo Moreira Mota Walmir Freitas Ahda pionkoski Grilo, Alexandre de Assis Mota. An Analytical Method for Analysis of Large-Disturbance Stability of Induction Generators. Technical report, IEEE, 2007.

[4] General Electric Company. 3.6 mw series wind turbine. http://www.gepower.com/prod_serv/products/wind_turbines/en/36mw/index.htm.

[5] Cuiqing Du. VSC-HVDC for Industrial Power Systems. Master's thesis, Chalmers University of Technology, 2007.

[6] Rune Kristian Mork Steinar Gjerve Svein Losnedal Øystein Kirkeluten Erik Bruun, Ragnar Mangelrød. *FIKS, Funksjonskrav i kraftsystemet*. Statnett SF, 2008.

[7] H. Beneke G. Böhmeke, R. Boldt. Geared drive intermediate solutions, comparison of design features and operating economics. In *Europ. Wind Energy Conf.*, pages 664–667, 1997.

[8] A. Gavrilovic. Ac/dc system strength as indicated by short circuit ratios.

[9] The ABB Group. HVCD Light. http://www.abb.no/, search "hvdc light".

[10] The ABB Group. Submarine XPLE cables up to 420 kV AC. http://www.abb.com/product/db0003db002618/c12573e7003302adc1256bdc00421ed7.aspx.

[11] The ABB Group. XPLE Cable Systems.

[12] Z. Chen H. Li. Overview of different wind generator systems and their comparison. Technical report, Institute of Energy Technology, Alborg University, 2007.

[13] L. Söder H.F. Latorre, M. Ghandhari. Active and reactive power control of a VSC-HVdc. Technical report, SienceDirect, 2008.

[14] A.L. Rogers J.F. Manwell, J.G. McGowan. *Wind Energy Explaned*. John Wiley & Sons, LTD, 2002.

[15] Prabha Kundur. *Power System Stability and Control*. McGraw-Hill, Inc, 1993.

[16] Bjarne R. Andresen Lie Xu. Grid Connection of Large Offshore Wind Farms Using HVDC. Technical report, Wiley Interscience, 2007.

[17] Stefan Lundberg. Configuration study of large wind parks. Master's thesis, Chalmers University of technology, 2003.

[18] Roy Maclean. Electrical System Design for the Proposed One Gigawatt Beatrice Offshore Wind Farm. Master's thesis, University of Strathclyde, 2004.

[19] Timo Vekara Martti Hokkanen, Heikki J. Salminen. A Short Review Of Models For Grid-Connected Doubly-Fed Variable Speed Wind Turbines. Technical report, University of Vaasa, 2004.

[20] Brian K. Johnsen Michael P. Bahrman. The ABCs of HVDC Transmission Technology. *IEEE Power & Energy Magazine*, 5(2), 2007.

[21] Juan J. Sanchez-Gasca Nicholas W. Miller, William W. Price. Dynamic Modeling of GE 1.5 and 3.6 Wind Turbine-Generators. Technical report, GE-Power Systems Energy Consulting, 2003.

[22] G. Smith P. Gardner, L. Craig. *Electrical System for Offshore Wind Farms*. Garrad Hassan & Partners, 1997.

[23] Rik W. S. Müller, M Deicke. Doubly Fed Induction Generator System, 2002.

[24] SIEMENS. *$PSS^{TM}E$ 31.0, Online Documentation*, 2007.

[25] Sigmund Smøttebråten. Hvdc Light teknologi for offshore anvendelser. Master's thesis, Norges teknisk-naturvitenskaplige universitet, 1999.

[26] Knut Magnus Sommerfelt. Offshore Wind Power in the North Sea. Master's thesis, Chalmers University of technology, 2003.

[27] Statkraft.

[28] Trond Toftevåg. private conversations.

[29] J.H. den Boon W.L. Kling, R.L. Hendriks. Advanced Transmission Solutions for Offshore Wind Frams. Technical report, IEEE, 2008.

[30] B. Pääjarvi Y. Jiang-Häfner, M. Hyttinen. On the Short Circuit Current Contribution of HVDC Light.

A Input data

A.1 Load flow input data - GE 3.6 Wind Turbine

Table 11: Individual WTG load flow data

Generator rating	4 MVA
Pmax	3.6 MVA
Pmin	0.5 MVA
Qmax	1.74
Qmin	-1.74
Terminal voltage	4160
Unit transformer rating	4 MVA
Leakage reactance	6%

```
     1804,'1 ',    3.600,    0.000,    1.740,   -1.740,1.00000,    2,    4.000, 0.00000E+0, 8.00000E-1,
0.00000E+0, 0.00000E+0,1.00000,1,  100.0,    3.600,    0.500,   1,1.0000,   ,    ,   ,    ,   , ,2, 0.9000
```

Figure 64: Copy of PSS/E load flow input data for the WTG

```
18184,  1804,    0,'1 ',1,1,1, 0.00000E+0, 0.00000E+0,2,'          ',1,   1,1.0000
 0.00000E+0, 1.50000E+0,    4.00
1.00000,   0.000,   0.000,    4.00,    0.00,    0.00, 0,    0, 1.10000, 0.90000, 1.10000, 0.90000,  33, 0, 0.00000, 0.00000
1.00000,   0.000
```

Figure 65: Copy of PSS/E load flow input data for the WTG equivalent transformer

X_{source} in the load flow model, has to be the same as X_{eq} in the dynamical model. Since X_{eq} was given by [24], X_{source} was set to 0.8 pu.

A.2 Generator/converter inputdata - GE 3.6 Wind Turbine

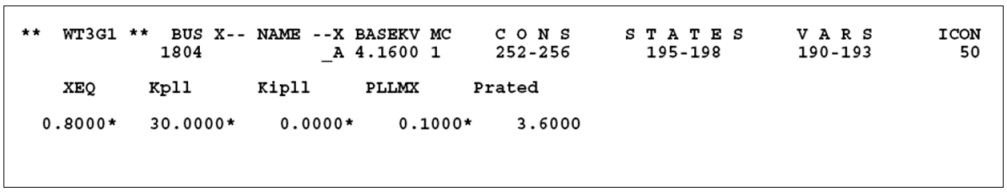

```
**  WT3G1 **  BUS X-- NAME --X BASEKV MC    C O N S     S T A T E S     V A R S      ICON
             1804           _A 4.1600 1    252-256       195-198       190-193        50

    XEQ     Kpll      Kipll     PLLMX     Prated

  0.8000*   30.0000*    0.0000*    0.1000*    3.6000
```

Figure 66: Copy of PSS/E generator/converter input data for the WTG

Inputdat that is marked with * are data from [24], the others are datas from [21].

A.3 Electrical converter inputdata - GE 3.6 Wind Turbine

```
**  WT3E1 **  BUS X-- NAME --X BASEKV MC    C O N S     S T A T E S     V A R S      I C
O N S
            1804           _A 4.1600 1    1999-2029      897-906       751-757
390-395

     TFV      KPV      KIV       XC       TFP       KPP       KIP
   0.1500*  18.0000*   5.0000*   0.0500*   0.0500*   3.0000*   0.6000*

     PMX      PMN       QMX       QMN      IPMAX     TRV       RPMX
   1.1200*   0.1000*   0.4360   -0.4360    1.1500    0.0500*   0.4500*

     RPMN    T_POWER    KQi
  -0.4500*   5.0000*   0.0500

     VMINCL    VMAXCL    Kqv     XIQmin    XIQmax     Tv
   0.4700    1.3900   40.0000*  -0.5000* 0.4000*   0.0500

     Tp        Fn       Wpmin     Wp20
   0.0500*   1.0000*   0.6900*   0.7800*
     Wp40     Wp60      Pwp      Wp100
   0.9800*   1.1200*   0.7400*   1.2000*

              Remote controlled Bus #         3
              VARFLG =  1      VLTFLG =  0
              BUS FROM =    1804 BUS TO =   18184 ID = $$
```

Figure 67: Copy of PSS/E generator/converter input data for the WTG

Inputdat that is marked with * are datas from [24], the others are datas from [21].

QMX and QMN was changed from 0.432 to 0.436, data from [21], because the per unit value of the reactive power capability of each machine is 0.4359. IP_{max} was changed from 1.1 to 1.15, VMINCL was changed from 0.9 to 0.47 in AC/AC model, and VMAXCL was changed from 1.2 to 1.39 in both models. This values was changed because at maximum power generation the limits were exeeded. VNINCL was changed from 0.9 to 1.12 in the AC/DC model. This was done because this gave a better regulation after a disturbance.

A.4 Mechanical control model input data - GE 3.6 Wind Turbine

** WT3T1 **	BUS X-- NAME --X	BASEKV	MC	C O N S	S T A T E S	V A R S	ICON
	1804	_A	4.1600 1	4173-4180	1665-1668	1392-1396	785

Vw	H	DAMP	Kaero	Theta2
1.2500*	5.1900	0.0000*	0.0070*	21.9800*

Htfrac	Freq1	DSHAFT
0.8266	2.5968	1.5000*

Figure 68: Copy of PSS/E mechanical control input data for the WTG

Inputdat that is marked with * are datas from [24], the others are datas from [21].

H_{tfrac} and F_{freq1} has to be calculated based on equations given in the PSS/E user manual [24]. These are given by

$$H_{fraq} = \frac{H_t}{H} = \frac{4.29}{5.19} \approx 0.8266 \tag{20}$$

$$F_{freq1} = \sqrt{\frac{K}{2 \times H_t \times (H_g/)}} \times 2\pi = \sqrt{\frac{K_{tg} \times \omega_{base}}{2 \times H_t \times (H_g/)}} \times \frac{2}{\pi} = \sqrt{\frac{296.7 \times 1.335}{2 \times 2.29 \times (0.9/5.19)}} \times \frac{2}{\pi} \approx 2.5968 \tag{21}$$

H_t named H, and K is given by $K_{tg} \times \omega_{base}$ in the GE 3.6 WTG documentation [21].

A.5 Pitch control input data - GE 3.6 Wind Turbine

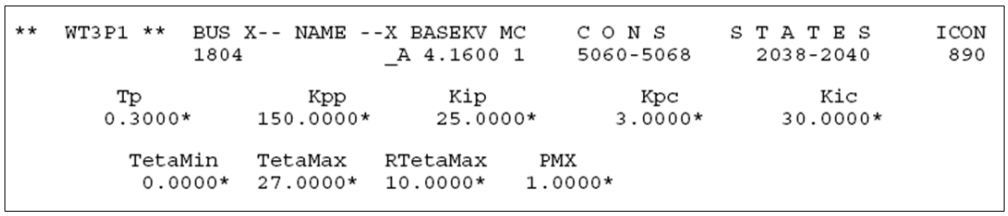

```
**  WT3P1 **  BUS X-- NAME --X BASEKV MC    C O N S     S T A T E S     ICON
              1804           _A 4.1600 1    5060-5068     2038-2040      890

        Tp             Kpp         Kip            Kpc           Kic
      0.3000*      150.0000*    25.0000*       3.0000*      30.0000*

         TetaMin   TetaMax   RTetaMax    PMX
          0.0000*  27.0000*  10.0000*   1.0000*
```

Figure 69: Copy of PSS/E pitch control inputdata for the WTG

Inputdat that is marked with * are datas from [24], the others are datas from [21]

A.6 Load flow input data - Equivalent Wind Turbine

.

Table 12: Equivalent WTG load flow data

Generator rating	32 MVA
Pmax	28.8 MVA
Pmin	4 MVA
Qmax	13.95
Qmin	-13.95
Terminal voltage	4160
Unit transformer rating	32 MVA
Leakage reactance	6%

```
     11,'1 ',   28.800,    0.000,   13.950,  -13.950,1.00000,    3,   32.000, 0.00000E+0, 8.00000E-1,
0.00000E+0, 0.00000E+0,1.00000,1,  100.0,   28.800,    0.500,  1,1.0000,   ,    ,   ,    ,   , ,2, 0.9000
```

Figure 70: Copy of PSS/E load flow input data for the WTG

```
  111,   11,    0,'1 ',1,1,1, 0.00000E+0, 0.00000E+0,2,'          ',1,   1,1.0000
 0.00000E+0, 1.87500E-1,   32.00
1.00000,  0.000,  0.000,   32.00,    0.00,    0.00, 0,    0, 1.10000, 0.90000, 1.10000, 0.90000,  33, 0, 0.00000, 0.00000
1.00000,  0.000
```

Figure 71: Copy of PSS/E load flow input data for the WTG equivalent transformer

A.7 Input data - Transformators

```
   3,    1,    0,'1 ',1,1,1, 0.00000E+0, 0.00000E+0,1,'          ',1,   1,1.0000
 2.91667E-4, 1.41637E-2,  1200.00
1.00000,   0.000,   0.000,  1200.00,     0.00,     0.00, 0,     0, 1.10000, 0.90000, 1.05000, 0.95000,  33, 0, 0.00000, 0.00000
1.00000,   0.000
```

Figure 72: Copy of PSS/E load flow input data for the high voltage transformers

The value of the reactance and the impedance are given in system per unit.

A.8 Input data - SVC

```
2,'1 ',    0.000,    0.000,  570.000, -570.000,1.00000,    0,  570.000, 0.00000E+0, 1.00000E+0,
        0.00000E+0, 0.00000E+0,1.00000,1,  100.0,    0.000,    0.000,  1,1.0000
```

Figure 73: Copy of PSS/E load flow input data for the SVC

```
** CSVGN5 **  BUS X-- NAME --X BASEKV MC    C O N S     S T A T E S     VAR   I C O N S
               2 LAND         420.00 1       3-16          3-6           1      1-2

      MBASE  REMOTE BUS    TS1    VEMAX    TS2     TS3     TS4     TS5
      570.0          2    0.000   0.150   0.000   0.700   0.000   0.700

         KSVS     KSD     BMAX   B'MAX   B'MIN    BMIN    TS6      DV
         50.0     0.0    1.000   1.000  -1.100  -1.100   0.030   0.250
```

Figure 74: Copy of PSS/E SVC model inputdata

A.9 Input data - Transformers

```
   3,    1,    0,'1 ',1,1,1, 0.00000E+0, 0.00000E+0,1,'          ',1,   1,1.0000
 2.91667E-4, 1.41637E-2,  1200.00
1.00000,   0.000,   0.000,  1200.00,     0.00,     0.00, 0,     0, 1.10000, 0.90000, 1.05000, 0.95000,  33, 0, 0.00000, 0.00000
1.00000,   0.000
```

Figure 75: Copy of PSS/E load flow input data for the transformers

The gain K_{SVS} is set to 50. A low value of the gain reduce the amplitudes of the ocillations after a fault.

A.10 Input data - Swing maschine

```
** GENCLS **  BUS X-- NAME --X BASEKV MC    C O N S     S T A T E S
                4 SWING        300.00 1       1-2           1-2

     MBASE     Z S O R C E          X T R A N       GENTAP      H     DAMP
    9999.0  0.00000+J 1.00000  0.00000+J 0.00000  1.00000    0.00   0.000
```

Figure 76: Copy of PSS/E GENCLS model inputdata

B Load flow results AC/AC

B.1 Generator VAR limit checking report, without SVC

GENERATORS AT VAR LIMITS:

BUS#	X-- NAME --X	BASKV	# MACH ON/OFF	TYP	MW	MVAR	QMAX	QMIN	VSCHED	VACTUAL	X----- REMOTE BUS ------X BUS#	X-- NAME --X	BASKV	MVABASE	ZONE	AREA
SWING																
1301		4.1600	1 0	-2	3.6	-7.4	1.7	-1.7	1.0000	1.0000	3	TRAFOR-H@GSP420.00		4.0	1	1
1302		4.1600	1 0	-2	3.6	-7.4	1.7	-1.7	1.0000	1.0000	3	TRAFOR-H@GSP420.00		4.0	1	1
1303		4.1600	1 0	-2	3.6	-7.4	1.7	-1.7	1.0000	1.0000	3	TRAFOR-H@GSP420.00		4.0	1	1
1304		4.1600	1 0	-2	3.6	-7.4	1.7	-1.7	1.0000	1.0000	3	TRAFOR-H@GSP420.00		4.0	1	1
1305		4.1600	1 0	-2	3.6	-7.4	1.7	-1.7	1.0000	1.0000	3	TRAFOR-H@GSP420.00		4.0	1	1
1306		4.1600	1 0	-2	3.6	-7.4	1.7	-1.7	1.0000	1.0000	3	TRAFOR-H@GSP420.00		4.0	1	1
1307		4.1600	1 0	-2	3.6	-7.4	1.7	-1.7	1.0000	1.0000	3	TRAFOR-H@GSP420.00		4.0	1	1
1308		4.1600	1 0	-2	3.6	-7.4	1.7	-1.7	1.0000	1.0000	3	TRAFOR-H@GSP420.00		4.0	1	1
1401		4.1600	1 0	-2	3.6	-7.4	1.7	-1.7	1.0000	1.0000	3	TRAFOR-H@GSP420.00		4.0	1	1
1402	_74	4.1600	1 0	-2	3.6	-7.4	1.7	-1.7	1.0000	1.0000	3	TRAFOR-H@GSP420.00		4.0	1	1
1403	_64	4.1600	1 0	-2	3.6	-7.4	1.7	-1.7	1.0000	1.0000	3	TRAFOR-H@GSP420.00		4.0	1	1
1404	_54	4.1600	1 0	-2	3.6	-7.4	1.7	-1.7	1.0000	1.0000	3	TRAFOR-H@GSP420.00		4.0	1	1
1405	_44	4.1600	1 0	-2	3.6	-7.4	1.7	-1.7	1.0000	1.0000	3	TRAFOR-H@GSP420.00		4.0	1	1
1406	_34	4.1600	1 0	-2	3.6	-7.4	1.7	-1.7	1.0000	1.0000	3	TRAFOR-H@GSP420.00		4.0	1	1
1407	_24	4.1600	1 0	-2	3.6	-7.4	1.7	-1.7	1.0000	1.0000	3	TRAFOR-H@GSP420.00		4.0	1	1
1408	_14	4.1600	1 0	-2	3.6	-7.4	1.7	-1.7	1.0000	1.0000	3	TRAFOR-H@GSP420.00		4.0	1	1
1501	_G4	4.1600	1 0	-2	3.6	-7.4	1.7	-1.7	1.0000	1.0000	3	TRAFOR-H@GSP420.00		4.0	1	1
1502	_F4	4.1600	1 0	-2	3.6	-7.4	1.7	-1.7	1.0000	1.0000	3	TRAFOR-H@GSP420.00		4.0	1	1
1503	_E4	4.1600	1 0	-2	3.6	-7.4	1.7	-1.7	1.0000	1.0000	3	TRAFOR-H@GSP420.00		4.0	1	1
1504	_D4	4.1600	1 0	-2	3.6	-7.4	1.7	-1.7	1.0000	1.0000	3	TRAFOR-H@GSP420.00		4.0	1	1
1505	_C4	4.1600	1 0	-2	3.6	-7.4	1.7	-1.7	1.0000	1.0000	3	TRAFOR-H@GSP420.00		4.0	1	1
1506	_B4	4.1600	1 0	-2	3.6	-7.4	1.7	-1.7	1.0000	1.0000	3	TRAFOR-H@GSP420.00		4.0	1	1
1507	_A4	4.1600	1 0	-2	3.6	-7.4	1.7	-1.7	1.0000	1.0000	3	TRAFOR-H@GSP420.00		4.0	1	1
1508	_84	4.1600	1 0	-2	3.6	-7.4	1.7	-1.7	1.0000	1.0000	3	TRAFOR-H@GSP420.00		4.0	1	1
1601	_W4	4.1600	1 0	-2	3.6	-7.4	1.7	-1.7	1.0000	1.0000	3	TRAFOR-H@GSP420.00		4.0	1	1
1602	_V4	4.1600	1 0	-2	3.6	-7.4	1.7	-1.7	1.0000	1.0000	3	TRAFOR-H@GSP420.00		4.0	1	1
1603	_U4	4.1600	1 0	-2	3.6	-7.4	1.7	-1.7	1.0000	1.0000	3	TRAFOR-H@GSP420.00		4.0	1	1
1604	_T4	4.1600	1 0	-2	3.6	-7.4	1.7	-1.7	1.0000	1.0000	3	TRAFOR-H@GSP420.00		4.0	1	1
1605	_S4	4.1600	1 0	-2	3.6	-7.4	1.7	-1.7	1.0000	1.0000	3	TRAFOR-H@GSP420.00		4.0	1	1
1606	_R4	4.1600	1 0	-2	3.6	-7.4	1.7	-1.7	1.0000	1.0000	3	TRAFOR-H@GSP420.00		4.0	1	1
1607	_Q4	4.1600	1 0	-2	3.6	-7.4	1.7	-1.7	1.0000	1.0000	3	TRAFOR-H@GSP420.00		4.0	1	1
1608	_P4	4.1600	1 0	-2	3.6	-7.4	1.7	-1.7	1.0000	1.0000	3	TRAFOR-H@GSP420.00		4.0	1	1
1701	_A4	4.1600	1 0	-2	3.6	-7.4	1.7	-1.7	1.0000	1.0000	3	TRAFOR-H@GSP420.00		4.0	1	1
1702	_A4	4.1600	1 0	-2	3.6	-7.4	1.7	-1.7	1.0000	1.0000	3	TRAFOR-H@GSP420.00		4.0	1	1
1703	_A4	4.1600	1 0	-2	3.6	-7.4	1.7	-1.7	1.0000	1.0000	3	TRAFOR-H@GSP420.00		4.0	1	1
1704	_A4	4.1600	1 0	-2	3.6	-7.4	1.7	-1.7	1.0000	1.0000	3	TRAFOR-H@GSP420.00		4.0	1	1
1705	_A4	4.1600	1 0	-2	3.6	-7.4	1.7	-1.7	1.0000	1.0000	3	TRAFOR-H@GSP420.00		4.0	1	1
1706	_A4	4.1600	1 0	-2	3.6	-7.4	1.7	-1.7	1.0000	1.0000	3	TRAFOR-H@GSP420.00		4.0	1	1
1707	_A4	4.1600	1 0	-2	3.6	-7.4	1.7	-1.7	1.0000	1.0000	3	TRAFOR-H@GSP420.00		4.0	1	1
1708	_4	4.1600	1 0	-2	3.6	-7.4	1.7	-1.7	1.0000	1.0000	3	TRAFOR-H@GSP420.00		4.0	1	1
1801	_A4	4.1600	1 0	-2	3.6	-7.4	1.7	-1.7	1.0000	1.0000	3	TRAFOR-H@GSP420.00		4.0	1	1
1802	_A4	4.1600	1 0	-2	3.6	-7.4	1.7	-1.7	1.0000	1.0000	3	TRAFOR-H@GSP420.00		4.0	1	1
1803	_A4	4.1600	1 0	-2	3.6	-7.4	1.7	-1.7	1.0000	1.0000	3	TRAFOR-H@GSP420.00		4.0	1	1
1804	_A4	4.1600	1 0	-2	3.6	-7.4	1.7	-1.7	1.0000	1.0000	3	TRAFOR-H@GSP420.00		4.0	1	1
1805	_A4	4.1600	1 0	-2	3.6	-7.4	1.7	-1.7	1.0000	1.0000	3	TRAFOR-H@GSP420.00		4.0	1	1
1806	_A4	4.1600	1 0	-2	3.6	-7.4	1.7	-1.7	1.0000	1.0000	3	TRAFOR-H@GSP420.00		4.0	1	1
1807	_A4	4.1600	1 0	-2	3.6	-7.4	1.7	-1.7	1.0000	1.0000	3	TRAFOR-H@GSP420.00		4.0	1	1
1808	_A4	4.1600	1 0	-2	3.6	-7.4	1.7	-1.7	1.0000	1.0000	3	TRAFOR-H@GSP420.00		4.0	1	1
1901	_A4	4.1600	1 0	-2	3.6	-7.4	1.7	-1.7	1.0000	1.0000	3	TRAFOR-H@GSP420.00		4.0	1	1
1902	_A4	4.1600	1 0	-2	3.6	-7.4	1.7	-1.7	1.0000	1.0000	3	TRAFOR-H@GSP420.00		4.0	1	1
1903	_A4	4.1600	1 0	-2	3.6	-7.4	1.7	-1.7	1.0000	1.0000	3	TRAFOR-H@GSP420.00		4.0	1	1
1904	_A4	4.1600	1 0	-2	3.6	-7.4	1.7	-1.7	1.0000	1.0000	3	TRAFOR-H@GSP420.00		4.0	1	1
1905	_A4	4.1600	1 0	-2	3.6	-7.4	1.7	-1.7	1.0000	1.0000	3	TRAFOR-H@GSP420.00		4.0	1	1
1906	_A4	4.1600	1 0	-2	3.6	-7.4	1.7	-1.7	1.0000	1.0000	3	TRAFOR-H@GSP420.00		4.0	1	1
1907	_A4	4.1600	1 0	-2	3.6	-7.4	1.7	-1.7	1.0000	1.0000	3	TRAFOR-H@GSP420.00		4.0	1	1
1908	_A4	4.1600	1 0	-2	3.6	-7.4	1.7	-1.7	1.0000	1.0000	3	TRAFOR-H@GSP420.00		4.0	1	1
2001	_A4	4.1600	1 0	-2	3.6	-7.4	1.7	-1.7	1.0000	1.0000	3	TRAFOR-H@GSP420.00		4.0	1	1
2002	_A4	4.1600	1 0	-2	3.6	-7.4	1.7	-1.7	1.0000	1.0000	3	TRAFOR-H@GSP420.00		4.0	1	1
2003	_A4	4.1600	1 0	-2	3.6	-7.4	1.7	-1.7	1.0000	1.0000	3	TRAFOR-H@GSP420.00		4.0	1	1
2004	_A4	4.1600	1 0	-2	3.6	-7.4	1.7	-1.7	1.0000	1.0000	3	TRAFOR-H@GSP420.00		4.0	1	1
2005	_A4	4.1600	1 0	-2	3.6	-7.4	1.7	-1.7	1.0000	1.0000	3	TRAFOR-H@GSP420.00		4.0	1	1
2006	_A4	4.1600	1 0	-2	3.6	-7.4	1.7	-1.7	1.0000	1.0000	3	TRAFOR-H@GSP420.00		4.0	1	1
2007	_A4	4.1600	1 0	-2	3.6	-7.4	1.7	-1.7	1.0000	1.0000	3	TRAFOR-H@GSP420.00		4.0	1	1
2008	_A4	4.1600	1 0	-2	3.6	-7.4	1.7	-1.7	1.0000	1.0000	3	TRAFOR-H@GSP420.00		4.0	1	1
2101	_A4	4.1600	1 0	-2	3.6	-7.4	1.7	-1.7	1.0000	1.0000	3	TRAFOR-H@GSP420.00		4.0	1	1
2102	_A4	4.1600	1 0	-2	3.6	-7.4	1.7	-1.7	1.0000	1.0000	3	TRAFOR-H@GSP420.00		4.0	1	1
2103	_A4	4.1600	1 0	-2	3.6	-7.4	1.7	-1.7	1.0000	1.0000	3	TRAFOR-H@GSP420.00		4.0	1	1
2104	_A4	4.1600	1 0	-2	3.6	-7.4	1.7	-1.7	1.0000	1.0000	3	TRAFOR-H@GSP420.00		4.0	1	1
2105	_A4	4.1600	1 0	-2	3.6	-7.4	1.7	-1.7	1.0000	1.0000	3	TRAFOR-H@GSP420.00		4.0	1	1
2106	_A4	4.1600	1 0	-2	3.6	-7.4	1.7	-1.7	1.0000	1.0000	3	TRAFOR-H@GSP420.00		4.0	1	1
2107	_A4	4.1600	1 0	-2	3.6	-7.4	1.7	-1.7	1.0000	1.0000	3	TRAFOR-H@GSP420.00		4.0	1	1
2108	_A4	4.1600	1 0	-2	3.6	-7.4	1.7	-1.7	1.0000	1.0000	3	TRAFOR-H@GSP420.00		4.0	1	1
2201	_A4	4.1600	1 0	-2	3.6	-7.4	1.7	-1.7	1.0000	1.0000	3	TRAFOR-H@GSP420.00		4.0	1	1
2202	_A4	4.1600	1 0	-2	3.6	-7.4	1.7	-1.7	1.0000	1.0000	3	TRAFOR-H@GSP420.00		4.0	1	1
2203	_A4	4.1600	1 0	-2	3.6	-7.4	1.7	-1.7	1.0000	1.0000	3	TRAFOR-H@GSP420.00		4.0	1	1
2204	_A4	4.1600	1 0	-2	3.6	-7.4	1.7	-1.7	1.0000	1.0000	3	TRAFOR-H@GSP420.00		4.0	1	1
2205	_A4	4.1600	1 0	-2	3.6	-7.4	1.7	-1.7	1.0000	1.0000	3	TRAFOR-H@GSP420.00		4.0	1	1
2206	_A4	4.1600	1 0	-2	3.6	-7.4	1.7	-1.7	1.0000	1.0000	3	TRAFOR-H@GSP420.00		4.0	1	1
2207	_A4	4.1600	1 0	-2	3.6	-7.4	1.7	-1.7	1.0000	1.0000	3	TRAFOR-H@GSP420.00		4.0	1	1
2208	_A4	4.1600	1 0	-2	3.6	-7.4	1.7	-1.7	1.0000	1.0000	3	TRAFOR-H@GSP420.00		4.0	1	1
SUBSYSTEM TOTALS					288.0	-592.9	139.5	-139.5						320.0		

B.2 Voltage limit checking report for busbar voltages between 0.9 and 1.05 pu, SVC=100 MVA

BUSES WITH VOLTAGE GREATER THAN 1.0500:

BUS#	X-- NAME --X	BASKV	AREA	V(PU)	V(KV)	BUS#	X-- NAME --X	BASKV	AREA	V(PU)	V(KV)
2	LAND	420.00	1	1.0976	461.01	3	TRAPOR-HøGSP4	420.00	1	1.1031	463.30

BUSES WITH VOLTAGE LESS THAN 0.9000:

BUS#	X-- NAME --X	BASKV	AREA	V(PU)	V(KV)	BUS#	X-- NAME --X	BASKV	AREA	V(PU)	V(KV)

* NONE *

B.3 Load flow results at with P=0.5 MW and SVC=570 MVA

```
BUS      4 SWING       300.00 CKT     MW     MVAR     MVA   % 1.0000PU    0.00  X--- LOSSES ---X X---- AREA -----X X---- ZC
-----X      4
  FROM GENERATION                   -130.4   -40.5R  136.5   1 300.00KV              MW     MVAR    1                 1
  TO       2 LAND        420.00  1  -130.4   -40.5   136.5  11 1.0000LK             0.05    2.64    1                 1

 BUS      2 LAND        420.00 CKT     MW     MVAR     MVA   % 1.0063PU    1.04  X--- LOSSES ---X X---- AREA -----X X----
ZONE -----X      2
  FROM GENERATION                     0.0  -570.0L  570.0 100 422.64KV              MW     MVAR    1                 1
  TO       3 TRAFOR-HøGSP420.00  1   -65.2  -306.6   313.4  57                     0.13    0.22    1                 1
  TO       3 TRAFOR-HøGSP420.00  2   -65.2  -306.6   313.4  57                     0.13    0.22    1                 1
  TO       4 SWING       300.00  1   130.4    43.1   137.4  11 1.0000UN             0.05    2.64    1                 1

 BUS      3 TRAFOR-HøGSP420.00 CKT     MW     MVAR     MVA   % 1.0092PU    1.17  X--- LOSSES ---X X---- AREA -----X X----
ZONE -----X      3
                                                     423.86KV              MW     MVAR    1                 1
  TO       1 TRAFO-LAVSP 33.000  1  -130.7    519.7   535.9  45 1.0000LK             0.82   39.94    1                 1
  TO       2 LAND        420.00  1    65.4   -259.9   267.9  48                     0.13    0.22    1                 1
  TO       2 LAND        420.00  2    65.4   -259.9   267.9  48                     0.13    0.22    1                 1

 BUS      1 TRAFO-LAVSP 33.000 CKT     MW     MVAR     MVA   % 0.9368PU    2.39  X--- LOSSES ---X X---- AREA -----X X----
ZONE -----X      1
                                                     30.916KV              MW     MVAR    1                 1
  TO       3 TRAFOR-HøGSP420.00  1   131.5   -479.8   497.5  41 1.0000UN             0.82   39.94    1                 1
  TO     111           _A33.000  1    -3.7     13.5    14.0  41                     0.34    0.48    1                 1
  TO     221           _A33.000  1    -3.7     13.5    14.0  41                     0.34    0.48    1                 1
  TO     331           _A33.000  1    -3.7     13.5    14.0  41                     0.34    0.48    1                 1
  TO     441           _A33.000  1    -3.7     13.5    14.0  41                     0.34    0.48    1                 1
  TO     551           _A33.000  1    -3.7     13.5    14.0  41                     0.34    0.48    1                 1
  TO     661           _A33.000  1    -3.7     13.5    14.0  41                     0.34    0.48    1                 1
  TO     771           _A33.000  1    -3.7     13.8    14.3  42                     0.28    0.36    1                 1
  TO     881           _A33.000  1    -3.7     13.8    14.3  42                     0.28    0.36    1                 1
  TO     991           _A33.000  1    -3.7     13.8    14.3  42                     0.28    0.36    1                 1
  TO   10101           _A33.000  1    -3.7     13.8    14.3  42                     0.28    0.36    1                 1
  TO   11111           _A33.000  1    -3.7     13.8    14.3  42                     0.28    0.36    1                 1
  TO   12121           _A33.000  1    -3.7     13.8    14.3  42                     0.28    0.36    1                 1
  TO   13131             33.000  1    -3.9     13.9    14.5  42                     0.03    0.06    1                 1
  TO   14141           _933.000  1    -3.9     13.9    14.5  42                     0.03    0.06    1                 1
  TO   15151           _H33.000  1    -3.9     13.9    14.5  42                     0.03    0.06    1                 1
  TO   16161           _X33.000  1    -3.9     13.9    14.5  42                     0.03    0.06    1                 1
  TO   17171           _A33.000  1    -3.9     13.9    14.5  42                     0.03    0.06    1                 1
  TO   18181           _A33.000  1    -3.9     13.9    14.5  42                     0.03    0.06    1                 1
  TO   19191           _A33.000  1    -3.9     13.9    14.5  42                     0.03    0.06    1                 1
  TO   20201           _A33.000  1    -3.9     13.9    14.5  42                     0.03    0.06    1                 1
  TO   21211           _A33.000  1    -3.9     13.9    14.5  42                     0.03    0.06    1                 1
  TO   22221           _A33.000  1    -3.9     13.9    14.5  42                     0.03    0.06    1                 1
  TO   23231           _A33.000  1    -3.7     13.8    14.3  42                     0.28    0.36    1                 1
  TO   24241           _A33.000  1    -3.7     13.8    14.3  42                     0.28    0.36    1                 1
  TO   25251           _A33.000  1    -3.7     13.8    14.3  42                     0.28    0.36    1                 1
  TO   26261           _A33.000  1    -3.7     13.8    14.3  42                     0.28    0.36    1                 1
  TO   27271           _A33.000  1    -3.7     13.8    14.3  42                     0.28    0.36    1                 1
  TO   28281           _A33.000  1    -3.7     13.8    14.3  42                     0.28    0.36    1                 1
  TO   29291           _A33.000  1    -3.7     13.5    14.0  41                     0.34    0.48    1                 1
  TO   30301           _A33.000  1    -3.7     13.5    14.0  41                     0.34    0.48    1                 1
  TO   31311           _A33.000  1    -3.7     13.5    14.0  41                     0.34    0.48    1                 1
  TO   32321           _A33.000  1    -3.7     13.5    14.0  41                     0.34    0.48    1                 1
  TO   33331           _A33.000  1    -3.7     13.5    14.0  41                     0.34    0.48    1                 1
  TO   34341           _A33.000  1    -3.7     13.5    14.0  41                     0.34    0.48    1                 1
  TO   35351           _A33.000  1    -3.7     13.5    14.0  41                     0.34    0.48    1                 1
```

B.4 Voltage limit checking report for busbar voltages between 0.9 and 1.05 pu,P=0.5 MW SVC=570 MVA

BUSES WITH VOLTAGE GREATER THAN 1.0500:

BUS#	X-- NAME	--X	BASKV	AREA	V(PU)	V(KV)	BUS#	X-- NAME	--X	BASKV	AREA	V(PU)	V(KV)
* NONE *													

BUSES WITH VOLTAGE LESS THAN 0.9000:

BUS#	X-- NAME	--X	BASKV	AREA	V(PU)	V(KV)	BUS#	X-- NAME	--X	BASKV	AREA	V(PU)	V(KV)
11		_A4.1600		1	0.8833	3.675	21		_A4.1600		1	0.8833	3.675
31		_A4.1600		1	0.8833	3.675	41		_A4.1600		1	0.8833	3.675
51		_A4.1600		1	0.8833	3.675	61		_A4.1600		1	0.8833	3.675
71		_A4.1600		1	0.8901	3.703	81		_A4.1600		1	0.8901	3.703
91		_A4.1600		1	0.8901	3.703	1001		_A4.1600		1	0.8901	3.703
1101		_A4.1600		1	0.8901	3.703	1201		_A4.1600		1	0.8901	3.703
2301		_A4.1600		1	0.8901	3.703	2401		_A4.1600		1	0.8901	3.703
2501		_A4.1600		1	0.8901	3.703	2601		_A4.1600		1	0.8901	3.703
2701		_A4.1600		1	0.8901	3.703	2801		_A4.1600		1	0.8901	3.703
2901		_A4.1600		1	0.8833	3.675	3001		_A4.1600		1	0.8833	3.675
3101		_A4.1600		1	0.8833	3.675	3201		_A4.1600		1	0.8833	3.675
3301		_A4.1600		1	0.8833	3.675	3401		_A4.1600		1	0.8833	3.675
3501		_A4.1600		1	0.8833	3.675							

B.5 Load flow results with P=3.6 MW and SVC=570 MVA

```
BUS      4 SWING       300.00 CKT     MW     MVAR     MVA   % 1.0000PU    0.00  X--- LOSSES ---X X---- AREA -----X X---- ZOI
-X     4
  FROM GENERATION                  -942.5    82.8R  946.1   9 300.00KV              MW     MVAR    1                1
  TO       2 LAND        420.00  1 -942.5    82.8   946.1  79 1.0000LK              2.61  126.78   1                1

 BUS      2 LAND        420.00 CKT     MW     MVAR     MVA   % 1.0000PU    7.69  X--- LOSSES ---X X---- AREA -----X X---- ZO
--X      2
  FROM GENERATION                     0.0  -234.1R  234.1  41 420.00KV              MW     MVAR    1                1
  TO       3 TRAFOR-HøGSP420.00  1 -472.5  -139.0   492.6  90                       6.83   10.99   1                1
  TO       3 TRAFOR-HøGSP420.00  2 -472.5  -139.0   492.6  90                       6.83   10.99   1                1
  TO       4 SWING       300.00  1  945.1    44.0   946.1  79 1.0000UN              2.61  126.78   1                1

 BUS      3 TRAFOR-HøGSP420.00 CKT     MW     MVAR     MVA   % 1.0073PU    9.13  X--- LOSSES ---X X---- AREA -----X X---- ZO
--X      3
                                                              423.05KV              MW     MVAR    1                1
  TO       1 TRAFO-LAVSP 33.000  1 -958.7    824.1  1264.2 105 1.0000LK              4.59  223.12   1                1
  TO       2 LAND        420.00  1  479.4   -412.0   632.1 114                       6.83   10.99   1                1
  TO       2 LAND        420.00  2  479.4   -412.0   632.1 114                       6.83   10.99   1                1

 BUS      1 TRAFO-LAVSP 33.000 CKT     MW     MVAR     MVA   % 0.9046PU   17.85  X--- LOSSES ---X X---- AREA -----X X---- ZO
--X      1
                                                               29.853KV             MW     MVAR    1                1
  TO       3 TRAFOR-HøGSP420.00  1  963.3   -601.0  1135.4  95 1.0000UN              4.59  223.12   1                1
  TO     111           _A33.000  1  -27.0     17.6    32.2  98                       1.81    2.55   1                1
  TO     221           _A33.000  1  -27.0     17.6    32.2  98                       1.81    2.55   1                1
  TO     331           _A33.000  1  -27.0     17.6    32.2  98                       1.81    2.55   1                1
  TO     441           _A33.000  1  -27.0     17.6    32.2  98                       1.81    2.55   1                1
  TO     551           _A33.000  1  -27.0     17.6    32.2  98                       1.81    2.55   1                1
  TO     661           _A33.000  1  -27.0     17.6    32.2  98                       1.81    2.55   1                1
  TO     771           _A33.000  1  -27.4     17.3    32.4  98                       1.45    1.88   1                1
  TO     881           _A33.000  1  -27.4     17.3    32.4  98                       1.45    1.88   1                1
  TO     991           _A33.000  1  -27.4     17.3    32.4  98                       1.45    1.88   1                1
  TO   10101           _A33.000  1  -27.4     17.3    32.4  98                       1.45    1.88   1                1
  TO   11111           _A33.000  1  -27.4     17.3    32.4  98                       1.45    1.88   1                1
  TO   12121           _A33.000  1  -27.4     17.3    32.4  98                       1.45    1.88   1                1
  TO   13131             33.000  1  -28.4     16.5    32.9 100                       0.16    0.30   1                1
  TO   14141           _933.000  1  -28.4     16.5    32.9 100                       0.16    0.30   1                1
  TO   15151           _H33.000  1  -28.4     16.5    32.9 100                       0.16    0.30   1                1
  TO   16161           _X33.000  1  -28.4     16.5    32.9 100                       0.16    0.30   1                1
  TO   17171           _A33.000  1  -28.4     16.5    32.9 100                       0.16    0.30   1                1
  TO   18181           _A33.000  1  -28.4     16.5    32.9 100                       0.16    0.30   1                1
  TO   19191           _A33.000  1  -28.4     16.5    32.9 100                       0.16    0.30   1                1
  TO   20201           _A33.000  1  -28.4     16.5    32.9 100                       0.16    0.30   1                1
  TO   21211           _A33.000  1  -28.4     16.5    32.9 100                       0.16    0.30   1                1
  TO   22221           _A33.000  1  -28.4     16.5    32.9 100                       0.16    0.30   1                1
  TO   23231           _A33.000  1  -27.4     17.3    32.4  98                       1.45    1.88   1                1
  TO   24241           _A33.000  1  -27.4     17.3    32.4  98                       1.45    1.88   1                1
  TO   25251           _A33.000  1  -27.4     17.3    32.4  98                       1.45    1.88   1                1
  TO   26261           _A33.000  1  -27.4     17.3    32.4  98                       1.45    1.88   1                1
  TO   27271           _A33.000  1  -27.4     17.3    32.4  98                       1.45    1.88   1                1
  TO   28281           _A33.000  1  -27.4     17.3    32.4  98                       1.45    1.88   1                1
  TO   29291           _A33.000  1  -27.0     17.6    32.2  98                       1.81    2.55   1                1
  TO   30301           _A33.000  1  -27.0     17.6    32.2  98                       1.81    2.55   1                1
  TO   31311           _A33.000  1  -27.0     17.6    32.2  98                       1.81    2.55   1                1
  TO   32321           _A33.000  1  -27.0     17.6    32.2  98                       1.81    2.55   1                1
  TO   33331           _A33.000  1  -27.0     17.6    32.2  98                       1.81    2.55   1                1
  TO   34341           _A33.000  1  -27.0     17.6    32.2  98                       1.81    2.55   1                1
  TO   35351           _A33.000  1  -27.0     17.6    32.2  98                       1.81    2.55   1                1
```

B.6 Voltage limit checking report for busbar voltages between 0.9 and 1.05 pu,P=3.6 MW SVC=570 MVA

BUSES WITH VOLTAGE GREATER THAN 1.0500:

BUS#	X-- NAME --X	BASKV	AREA	V(PU)	V(KV)	BUS#	X-- NAME --X	BASKV	AREA	V(PU)	V(KV)
					* NONE *						

BUSES WITH VOLTAGE LESS THAN 0.9000:

BUS#	X-- NAME --X	BASKV	AREA	V(PU)	V(KV)	BUS#	X-- NAME --X	BASKV	AREA	V(PU)	V(KV)
11	_A4.1600		1	0.8789	3.656	21	_A4.1600		1	0.8789	3.656
31	_A4.1600		1	0.8789	3.656	41	_A4.1600		1	0.8789	3.656
51	_A4.1600		1	0.8789	3.656	61	_A4.1600		1	0.8789	3.656
71	_A4.1600		1	0.8804	3.663	81	_A4.1600		1	0.8804	3.663
91	_A4.1600		1	0.8804	3.663	1001	_A4.1600		1	0.8804	3.663
1101	_A4.1600		1	0.8804	3.663	1201	_A4.1600		1	0.8804	3.663
1301	4.1600		1	0.8723	3.629	1302	4.1600		1	0.8722	3.628
1303	4.1600		1	0.8729	3.631	1304	4.1600		1	0.8734	3.633
1305	4.1600		1	0.8739	3.635	1306	4.1600		1	0.8751	3.640
1307	4.1600		1	0.8759	3.644	1308	4.1600		1	0.8763	3.645
1401	_4.1600		1	0.8723	3.629	1402	_74.1600		1	0.8722	3.628
1403	_64.1600		1	0.8729	3.631	1404	_54.1600		1	0.8734	3.633
1405	_44.1600		1	0.8739	3.635	1406	_34.1600		1	0.8751	3.640
1407	_24.1600		1	0.8759	3.644	1408	_14.1600		1	0.8763	3.645
1501	_G4.1600		1	0.8723	3.629	1502	_F4.1600		1	0.8722	3.628
1503	_E4.1600		1	0.8729	3.631	1504	_D4.1600		1	0.8734	3.633
1505	_C4.1600		1	0.8739	3.635	1506	_B4.1600		1	0.8751	3.640
1507	_A4.1600		1	0.8759	3.644	1508	_84.1600		1	0.8763	3.645
1601	_W4.1600		1	0.8723	3.629	1602	_V4.1600		1	0.8722	3.628
1603	_U4.1600		1	0.8729	3.631	1604	_T4.1600		1	0.8734	3.633
1605	_S4.1600		1	0.8739	3.635	1606	_R4.1600		1	0.8751	3.640
1607	_Q4.1600		1	0.8759	3.644	1608	_P4.1600		1	0.8763	3.645
1701	_A4.1600		1	0.8723	3.629	1702	_A4.1600		1	0.8722	3.628
1703	_A4.1600		1	0.8729	3.631	1704	_A4.1600		1	0.8734	3.633
1705	_A4.1600		1	0.8739	3.635	1706	_A4.1600		1	0.8751	3.640
1707	_A4.1600		1	0.8759	3.644	1708	_`4.1600		1	0.8763	3.645
1801	_A4.1600		1	0.8723	3.629	1802	_A4.1600		1	0.8722	3.628
1803	_A4.1600		1	0.8729	3.631	1804	_A4.1600		1	0.8734	3.633
1805	_A4.1600		1	0.8739	3.635	1806	_A4.1600		1	0.8752	3.641
1807	_A4.1600		1	0.8760	3.644	1808	_A4.1600		1	0.8764	3.646
1901	_A4.1600		1	0.8723	3.629	1902	_A4.1600		1	0.8722	3.628
1903	_A4.1600		1	0.8729	3.631	1904	_A4.1600		1	0.8734	3.633
1905	_A4.1600		1	0.8739	3.635	1906	_A4.1600		1	0.8751	3.640
1907	_A4.1600		1	0.8759	3.644	1908	_A4.1600		1	0.8763	3.645
2001	_A4.1600		1	0.8723	3.629	2002	_A4.1600		1	0.8722	3.628
2003	_A4.1600		1	0.8729	3.631	2004	_A4.1600		1	0.8734	3.633
2005	_A4.1600		1	0.8739	3.635	2006	_A4.1600		1	0.8751	3.640
2007	_A4.1600		1	0.8759	3.644	2008	_A4.1600		1	0.8763	3.645
2101	_A4.1600		1	0.8723	3.629	2102	_A4.1600		1	0.8722	3.628
2103	_A4.1600		1	0.8729	3.631	2104	_A4.1600		1	0.8734	3.633
2105	_A4.1600		1	0.8739	3.635	2106	_A4.1600		1	0.8751	3.640
2107	_A4.1600		1	0.8759	3.644	2108	_A4.1600		1	0.8763	3.645
2201	_A4.1600		1	0.8723	3.629	2202	_A4.1600		1	0.8722	3.628
2203	_A4.1600		1	0.8729	3.631	2204	_A4.1600		1	0.8734	3.633
2205	_A4.1600		1	0.8739	3.635	2206	_A4.1600		1	0.8751	3.640
2207	_A4.1600		1	0.8759	3.644	2208	_A4.1600		1	0.8763	3.645
2301	_A4.1600		1	0.8804	3.663	2401	_A4.1600		1	0.8804	3.663
2501	_A4.1600		1	0.8804	3.663	2601	_A4.1600		1	0.8804	3.663
2701	_A4.1600		1	0.8804	3.663	2801	_A4.1600		1	0.8804	3.663
2901	_A4.1600		1	0.8789	3.656	3001	_A4.1600		1	0.8789	3.656
3101	_A4.1600		1	0.8789	3.656	3201	_A4.1600		1	0.8789	3.656
3301	_A4.1600		1	0.8789	3.656	3401	_A4.1600		1	0.8789	3.656
3501	_A4.1600		1	0.8789	3.656						

B.7 Load flow results for the DC system with P=3.6 MW

```
BUS      9 SWING       300.00 CKT     MW     MVAR     MVA   % 1.0000PU    0.00  X--- LOSSES ---X X---- AREA -----X X---- ZONE ----
-X       9
  FROM GENERATION                   -938.7   -17.7R  938.8   9 300.00KV              MW     MVAR    1                1
  TO       1 LAND        400.00  1  -938.7   -17.7   938.8  78 1.0000LK    0.00LK    2.59  125.76    1                1

 BUS       1 LAND        400.00 CKT     MW     MVAR     MVA   % 1.0000PU    7.65  X--- LOSSES ---X X---- AREA -----X X---- ZONE ---
--X       1
                                                      400.00KV              MW     MVAR    1                1
  TO       3 PCC_1       400.00  1   -941.3   -43.5   942.3                 0.00     0.00    1                1
  TO       9 SWING       300.00  1    941.3    43.5   942.3  79 1.0000UN            2.59  125.76    1                1

 BUS       3 PCC_1       400.00 CKT     MW     MVAR     MVA   % 1.0000PU    7.65  X--- LOSSES ---X X---- AREA -----X X---- ZONE ---
--X       3
                                                      400.00KV              MW     MVAR    1                1
  TO       1 LAND        400.00  1    941.3    43.5   942.3                 0.00     0.00    1                1
  TO       5 LIGHT_1     416.00  1   -941.3   -43.5   942.3     1.0000RG            0.00   82.59    1                1

 BUS       5 LIGHT_1     416.00 CKT     MW     MVAR     MVA   % 1.0079PU   12.64  X--- LOSSES ---X X---- AREA -----X X---- ZONE ---
--X       5
  FROM GENERATION                    941.3   -59.2R  943.1  78 419.27KV              MW     MVAR    1                1
  TO SHUNT                             0.0  -185.3   185.3
  TO       3 PCC_1       400.00  1    941.3   126.1   949.7     1.0000UN            0.00   82.59    1                1

 BUS       6 LIGHT_2     416.00 CKT     MW     MVAR     MVA   % 1.0000PU    0.00  X--- LOSSES ---X X---- AREA -----X X---- ZONE ---
--X       6
  FROM GENERATION                   -979.0  -137.7H  988.6  81 416.00KV              MW     MVAR    1                1
  TO SHUNT                             0.0  -182.4   182.4
  TO       4 PCC_2       400.00  1   -979.0    44.7   980.0     1.0000UN            0.00   89.34    1                1

 BUS       4 PCC_2       400.00 CKT     MW     MVAR     MVA   % 1.0000PU    5.22  X--- LOSSES ---X X---- AREA -----X X---- ZONE ---
--X       4
                                                      400.00KV              MW     MVAR    1                1
  TO       2 TRAFO-HøGSP 400.00  1   -979.0    44.7   980.0                 0.00     0.00    1                1
  TO       6 LIGHT_2     416.00  1    979.0    44.7   980.0     1.0000RG            0.00   89.34    1                1

 BUS       2 TRAFO-HøGSP 400.00 CKT     MW     MVAR     MVA   % 1.0000PU    5.22  X--- LOSSES ---X X---- AREA -----X X---- ZONE ---
--X       2
                                                      400.00KV              MW     MVAR    1                1
  TO       4 PCC_2       400.00  1    979.0    44.7   980.0                 0.00     0.00    1                1
  TO       8 TRAFO-LAVSP 33.000  1   -979.0    44.7   980.0  82 1.0000UN            2.80  136.02    1                1

 BUS       8 TRAFO-LAVSP 33.000 CKT     MW     MVAR     MVA   % 1.0186PU   13.04  X--- LOSSES ---X X---- AREA -----X X---- ZONE ---
--X       8
                                                      33.615KV              MW     MVAR    1                1
  TO       2 TRAFO-HøGSP 400.00  1    981.8   180.7   998.3  83 1.0000LK            2.80  136.02    1                1
  TO     111             _A33.000  1    -27.8    -2.3    27.9  75                     1.04    1.46    1                1
  TO     221             _A33.000  1    -27.8    -2.3    27.9  75                     1.04    1.46    1                1
  TO     331             _A33.000  1    -27.8    -2.3    27.9  75                     1.04    1.46    1                1
  TO     441             _A33.000  1    -27.8    -2.3    27.9  75                     1.04    1.46    1                1
  TO     551             _A33.000  1    -27.8    -2.3    27.9  75                     1.04    1.46    1                1
  TO     661             _A33.000  1    -27.8    -2.3    27.9  75                     1.04    1.46    1                1
  TO     771             _A33.000  1    -28.0    -2.1    28.0  76                     0.84    1.09    1                1
  TO     881             _A33.000  1    -28.0    -2.1    28.0  76                     0.84    1.09    1                1
  TO     991             _A33.000  1    -28.0    -2.1    28.0  76                     0.84    1.09    1                1
  TO   10101             _A33.000  1    -28.0    -2.1    28.0  76                     0.84    1.09    1                1
  TO   11111             _A33.000  1    -28.0    -2.1    28.0  76                     0.84    1.09    1                1
  TO   12121             _A33.000  1    -28.0    -2.1    28.0  76                     0.84    1.09    1                1
  TO   13131               33.000  1    -28.5   -12.5    31.2  84                     0.12    0.21    1                1
  TO   14141             _933.000  1    -28.5   -12.5    31.2  84                     0.12    0.21    1                1
  TO   15151             _H33.000  1    -28.5   -12.5    31.2  84                     0.12    0.21    1                1
  TO   16161             _X33.000  1    -28.5   -12.5    31.2  84                     0.12    0.21    1                1
  TO   17171             _A33.000  1    -28.5   -12.5    31.2  84                     0.12    0.21    1                1
  TO   18181             _A33.000  1    -28.5   -12.5    31.2  84                     0.12    0.21    1                1
  TO   19191             _A33.000  1    -28.5   -12.5    31.2  84                     0.12    0.21    1                1
  TO   20201             _A33.000  1    -28.5   -12.5    31.2  84                     0.12    0.21    1                1
  TO   21211             _A33.000  1    -28.5   -12.5    31.2  84                     0.12    0.21    1                1
  TO   22221             _A33.000  1    -28.5   -12.5    31.2  84                     0.12    0.21    1                1
  TO   23231             _A33.000  1    -28.0    -2.1    28.0  76                     0.84    1.09    1                1
  TO   24241             _A33.000  1    -28.0    -2.1    28.0  76                     0.84    1.09    1                1
  TO   25251             _A33.000  1    -28.0    -2.1    28.0  76                     0.84    1.09    1                1
  TO   26261             _A33.000  1    -28.0    -2.1    28.0  76                     0.84    1.09    1                1
  TO   27271             _A33.000  1    -28.0    -2.1    28.0  76                     0.84    1.09    1                1
  TO   28281             _A33.000  1    -28.0    -2.1    28.0  76                     0.84    1.09    1                1
  TO   29291             _A33.000  1    -27.8    -2.3    27.9  75                     1.04    1.46    1                1
  TO   30301             _A33.000  1    -27.8    -2.3    27.9  75                     1.04    1.46    1                1
  TO   31311             _A33.000  1    -27.8    -2.3    27.9  75                     1.04    1.46    1                1
  TO   32321             _A33.000  1    -27.8    -2.3    27.9  75                     1.04    1.46    1                1
  TO   33331             _A33.000  1    -27.8    -2.3    27.9  75                     1.04    1.46    1                1
  TO   34341             _A33.000  1    -27.8    -2.3    27.9  75                     1.04    1.46    1                1
  TO   35351             _A33.000  1    -27.8    -2.3    27.9  75                     1.04    1.46    1                1
```

B.8 Voltage limit checking report for busbar voltages between 0.9 and 1.05 pu,P=3.6 MW

BUSES WITH VOLTAGE GREATER THAN 1.0500:

BUS#	X-- NAME --	X BASKV	AREA	V(PU)	V(KV)	BUS#	X-- NAME --	X BASKV	AREA	V(PU)	V(KV)
11	_A4.1600		1	1.0653	4.432	21	_A4.1600		1	1.0653	4.432
31	_A4.1600		1	1.0653	4.432	41	_A4.1600		1	1.0653	4.432
51	_A4.1600		1	1.0653	4.432	61	_A4.1600		1	1.0653	4.432
71	_A4.1600		1	1.0566	4.395	81	_A4.1600		1	1.0566	4.395
91	_A4.1600		1	1.0566	4.395	111	_A33.000		1	1.0607	35.001
221	_A33.000		1	1.0607	35.001	331	_A33.000		1	1.0607	35.001
441	_A33.000		1	1.0607	35.001	551	_A33.000		1	1.0607	35.001
661	_A33.000		1	1.0607	35.001	771	_A33.000		1	1.0519	34.713
881	_A33.000		1	1.0519	34.713	991	_A33.000		1	1.0519	34.713
1001	_A4.1600		1	1.0566	4.395	1101	_A4.1600		1	1.0566	4.395
1201	_A4.1600		1	1.0566	4.395	1302	4.1600		1	1.0506	4.370
1303	4.1600		1	1.0530	4.380	1304	4.1600		1	1.0550	4.389
1305	4.1600		1	1.0566	4.395	1306	4.1600		1	1.0586	4.404
1307	4.1600		1	1.0599	4.409	1308	4.1600		1	1.0606	4.412
1402	_74.1600		1	1.0506	4.370	1403	_64.1600		1	1.0530	4.380
1404	_54.1600		1	1.0550	4.389	1405	_44.1600		1	1.0566	4.395
1406	_34.1600		1	1.0586	4.404	1407	_24.1600		1	1.0599	4.409
1408	_14.1600		1	1.0606	4.412	1502	_F4.1600		1	1.0506	4.370
1503	_E4.1600		1	1.0530	4.380	1504	_D4.1600		1	1.0550	4.389
1505	_C4.1600		1	1.0566	4.395	1506	_B4.1600		1	1.0586	4.404
1507	_A4.1600		1	1.0599	4.409	1508	_84.1600		1	1.0606	4.412
1602	_V4.1600		1	1.0506	4.370	1603	_U4.1600		1	1.0530	4.380
1604	_T4.1600		1	1.0550	4.389	1605	_S4.1600		1	1.0566	4.395
1606	_R4.1600		1	1.0586	4.404	1607	_Q4.1600		1	1.0599	4.409
1608	_P4.1600		1	1.0606	4.412	1702	_A4.1600		1	1.0506	4.370
1703	_A4.1600		1	1.0530	4.380	1704	_A4.1600		1	1.0550	4.389
1705	_A4.1600		1	1.0566	4.395	1706	_A4.1600		1	1.0586	4.404
1707	_A4.1600		1	1.0599	4.409	1708	`4.1600		1	1.0606	4.412
1802	_A4.1600		1	1.0506	4.370	1803	_A4.1600		1	1.0530	4.380
1804	_A4.1600		1	1.0550	4.389	1805	_A4.1600		1	1.0566	4.395
1806	_A4.1600		1	1.0585	4.404	1807	_A4.1600		1	1.0599	4.409
1808	_A4.1600		1	1.0606	4.412	1902	_A4.1600		1	1.0506	4.370
1903	_A4.1600		1	1.0530	4.380	1904	_A4.1600		1	1.0550	4.389
1905	_A4.1600		1	1.0566	4.395	1906	_A4.1600		1	1.0586	4.404
1907	_A4.1600		1	1.0599	4.409	1908	_A4.1600		1	1.0606	4.412
2002	_A4.1600		1	1.0506	4.370	2003	_A4.1600		1	1.0530	4.380
2004	_A4.1600		1	1.0550	4.389	2005	_A4.1600		1	1.0566	4.395
2006	_A4.1600		1	1.0586	4.404	2007	_A4.1600		1	1.0599	4.409
2008	_A4.1600		1	1.0606	4.412	2102	_A4.1600		1	1.0506	4.370
2103	_A4.1600		1	1.0530	4.380	2104	_A4.1600		1	1.0550	4.389
2105	_A4.1600		1	1.0566	4.395	2106	_A4.1600		1	1.0586	4.404
2107	_A4.1600		1	1.0599	4.409	2108	_A4.1600		1	1.0606	4.412
2202	_A4.1600		1	1.0506	4.370	2203	_A4.1600		1	1.0530	4.380
2204	_A4.1600		1	1.0550	4.389	2205	_A4.1600		1	1.0566	4.395
2206	_A4.1600		1	1.0586	4.404	2207	_A4.1600		1	1.0599	4.409
2208	_A4.1600		1	1.0606	4.412	2301	_A4.1600		1	1.0566	4.395
2401	_A4.1600		1	1.0566	4.395	2501	_A4.1600		1	1.0566	4.395
2601	_A4.1600		1	1.0566	4.395	2701	_A4.1600		1	1.0566	4.395
2801	_A4.1600		1	1.0566	4.395	2901	_A4.1600		1	1.0653	4.432
3001	_A4.1600		1	1.0653	4.432	3101	_A4.1600		1	1.0653	4.432
3201	_A4.1600		1	1.0653	4.432	3301	_A4.1600		1	1.0653	4.432
3401	_A4.1600		1	1.0653	4.432	3501	_A4.1600		1	1.0653	4.432
10101	_A33.000		1	1.0519	34.713	11111	_A33.000		1	1.0519	34.713
12121	_A33.000		1	1.0519	34.713	23231	_A33.000		1	1.0519	34.713
24241	_A33.000		1	1.0519	34.713	25251	_A33.000		1	1.0519	34.713
26261	_A33.000		1	1.0519	34.713	27271	_A33.000		1	1.0519	34.713
28281	_A33.000		1	1.0519	34.713	29291	_A33.000		1	1.0607	35.001
30301	_A33.000		1	1.0607	35.001	31311	_A33.000		1	1.0607	35.001
32321	_A33.000		1	1.0607	35.001	33331	_A33.000		1	1.0607	35.001
34341	_A33.000		1	1.0607	35.001	35351	_A33.000		1	1.0607	35.001

BUSES WITH VOLTAGE LESS THAN 0.9000:

BUS#	X-- NAME --	X BASKV	AREA	V(PU)	V(KV)	BUS#	X-- NAME --	X BASKV	AREA	V(PU)	V(KV)

* NONE *